

**WATER BORNE TRANSPORT OF HIGH LEVEL NUCLEAR WASTE IN VERY DEEP BOREHOLE DISPOSAL OF HIGH LEVEL NUCLEAR WASTE** ARCHIVES


By  
**DION TUNICK CABECHE**  
B.S. Nuclear Science and Engineering, 2011  
Submitted to the

DEPARTMENT OF NUCLEAR SCIENCE AND ENGINEERING  
In Partial Fulfillment of the Requirements for the Degree of  
BACHELOR OF SCIENCE IN NUCLEAR SCIENCE AND ENGINEERING  
at the  
MASSACHUSETTS INSTITUTE OF TECHNOLOGY  
June, 2011


© 2011 Dion Cabeche. All rights reserved

The author hereby grants to MIT permission to reproduce and distribute publicly paper and electronic copies of this thesis document in whole or in part.

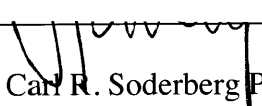
Signature of Author: \_\_\_\_\_

  
Dion Tunick Cabeche  
Department of Nuclear Science and Engineering  
May 20, 2011


Certified By: \_\_\_\_\_

  
Michael J. Driscoll  
Professor Emeritus of Nuclear Science and Engineering  
Thesis Supervisor

Certified By: \_\_\_\_\_

  
Jacopo Buongiorno  
Carl R. Soderberg Professor of Power Engineering  
Associate Professor of Nuclear Science and Engineering  
Thesis Reader

Accepted By: \_\_\_\_\_

  
Dennis Whyte  
Professor of Nuclear Science and Engineering  
Director, Plasma Surface Interactions Science Center  
Chairman, NSE Committee for Undergraduate Students

WATER BORNE TRANSPORT OF HIGH LEVEL NUCLEAR WASTE IN VERY  
DEEP BOREHOLE DISPOSAL OF HIGH LEVEL NUCLEAR WASTE

By

DION TUNICK CABECHE

Submitted to the Department of Nuclear Science and Engineering on May 20th, 2011.

In Partial Fulfillment of the Requirements for the Degree of

Bachelor of Science in Nuclear Science and Engineering

ABSTRACT

The purpose of this report is to examine the feasibility of the very deep borehole experiment and to determine if it is a reasonable method of storing high level nuclear waste for an extended period of time. The objective of this thesis is to determine the escape mechanisms of radionuclides and to determine if naturally occurring salinity gradients could counteract this phenomenon. Because of the large dependence on the water density, the relationship between water density and the salinity was measured and agreed with the literature values with a less than 1% difference. The resultant relationship between the density and salinity is a linear relationship with the molality, and dependent upon the number of ions of the dissolved salt (e.g.  $\text{CaCl}_2$  contains 3 and  $\text{NaCl}$  has 2).

From the data, it was calculated that within a borehole with a host rock porosity of  $10^{-5}$  Darcy, it would take approximately  $10^5$  years for the radionuclides to escape. As the rock porosity decreases, the escape time scale increases, and the escape fraction decreases exponentially. Due to the conservative nature of the calculations, the actual escape timescale would be closer to  $10^6$  years and dominated by I-129 in a reducing atmosphere. The expected borehole salinity values can offset the buoyancy effect due to a  $50^\circ\text{C}$  temperature increase.

Thesis Supervisor: Michael J. Driscoll

Title: Professor Emeritus of Nuclear Science and Engineering

## **Acknowledgements**

Professor Driscoll, thank you for your time and assistance in helping me get through this report, and thank you for your patience.

Thanks to Thomas McKrell for your assistance in helping me perform my experiments and for your help in acquiring the materials necessary for me to run my experiments.

Professor Buongiorno for helping me along the way and helping guide me in the right direction.

To my family, who supported me and helped me pull through and complete this project.

To my friends, who helped me structure my report and give me support.

To the Faculty and Staff of the Nuclear Science and Engineering Department, who have always helped me along the way.

And once more, my sincerest gratitude to Professors Driscoll and Buongiorno for their assistance.

## Table of Contents

<b>ABSTRACT</b> .....	<b>2</b>
<b>ACKNOWLEDGEMENTS</b> .....	<b>3</b>
<b>TABLE OF CONTENTS</b> .....	<b>4</b>
<b>LIST OF FIGURES</b> .....	<b>5</b>
<b>LIST OF TABLES</b> .....	<b>5</b>
<b>1. INTRODUCTION</b> .....	<b>6</b>
1.1 Deep Borehole Concept .....	8
1.2 Decay and Hazards of Nuclear Waste .....	10
1.3 Buoyancy Driven Nuclide Flow .....	11
<b>2. BACKGROUND INFORMATION</b> .....	<b>13</b>
2.1 Introduction .....	13
2.2 Waterborne Radionuclide Transport .....	13
2.3 Effects on Radionuclide Transport .....	15
2.4 Plume Effect.....	16
<b>3. DENSITY CALCULATIONS</b> .....	<b>18</b>
3.1 Introduction .....	18
3.2 Effect of Pressure and Temperature .....	18
3.3 Previous Salinity Experiments .....	20
3.4 Salinity vs. Density Experiments .....	22
<b>4. ANALYSIS</b> .....	<b>28</b>
4.1 Introduction .....	28
4.2 Radionuclide Movement Timescale .....	28
4.3 Radionuclide Escape Probability .....	30
4.4 Summary .....	32
<b>5. SUMMARY, CONCLUSIONS, AND RECOMMENDATIONS</b> .....	<b>34</b>
5.1 Summary and Conclusions .....	34
5.2 Future Work .....	35
<b>APPENDICES</b> .....	<b>37</b>
<b>REFERENCES</b> .....	<b>52</b>

## List of Figures

Figure 1-1 Deep Borehole Disposal Schematic.....	9
Figure 1-2 Log-Scale Thermal Power Released for Waste from a PWR for 1 MTIHM, 60,000 MWD/MTHM Burnup, and 10 Year Cooling.....	12
Figure 3-1 Change in Water Density as a Function of Salinity for Three Different Temperatures and Pressures.....	21
Figure 3-2 One Liter Pyrex Volumetric Flask.....	23
Figure 3-3 Cole-Palmer Low-Cost Specific Gravity Meter, 1.000 to 1.300 SGU, °C model.....	24
Figure 3-4 Results from Density Experiment (Molality).....	25
Figure 3-4 Results from Density Experiment (Mass).....	25
Figure 4-1 Escape Fraction of Iodine-129 as a Function of Time.....	32

## List of Tables

Table 4-1 Escape Fraction of Neptunium-237 by Water Transport.....	31
Table C-1 Cole-Palmer Low-Cost Specific Gravity Meter, 1.000 to 1.300 SGU, °C model Specifications.....	51

# 1 Introduction

The desire for cleaner energies has never been more apparent than in the past couple of decades. Fossil fuels dump nearly a trillion metric tonnes of carbon dioxide into the atmosphere each year, perhaps accelerating climate shifts significantly. As a result, much research has been performed on cleaner energies, such as wind, solar, and nuclear.

Among the available carbon-free energies, nuclear energy can run at full power all the time. In fact, most reactors operate at full power for about ninety percent of the year. The quantity of nuclear fuel on this planet, the lack of greenhouse gas emissions, and the high energy density of nuclear materials make nuclear energy a promising energy source for the future.

However, nuclear energy does come with a downside. After the fuel has been in the reactor typically for three fuel cycles of eighteen months each, the fuel assemblies, which include the cladding, the nuclear fuel, as well as the fission products are highly radioactive and must be stored so that these materials can decay without harming people or the environment. The materials that are the most dangerous are the fission products and the actinides, which can be very toxic and have long half-lives. These materials must be safely stored so that they can decay away while not adversely affecting the environment. Currently, the United States does not reprocess spent fuel. As of now, most

nuclear waste is contained at the reactor sites in dry casks. However, this is only meant to be a temporary solution. As such, safe means of disposing of the nuclear waste are a necessity.

Because of the cancellation of Yucca Mountain as a disposal facility for high level nuclear waste, a new initiative for storing nuclear materials has become necessary. One promising method to store these materials is in deep boreholes. Deep boreholes are deep holes in granite bedrock that can be up to several kilometers deep. The nuclear assemblies are encapsulated in casks to prevent corrosion and release of radioactivity into the surrounding ground water, and then placed in the boreholes. Due to the heat from the nuclear materials as well as the natural diffusion of the radionuclides into the ambient water, it is conceivable that the decay heat will produce a buoyant plume effect such that the ground water rises and consequently the radionuclides will rise with the heated water. Accordingly, the objective of this thesis is to evaluate this escape mechanism, and, in particular, to assess the ability of naturally occurring salinity gradients to counteract this phenomenon.

## 1.1 Deep Borehole Concept

Deep boreholes are a promising method for storing high level nuclear waste. The concept is that a hole is drilled into granite bedrock in relatively stable areas. These holes are around four to five kilometers deep. The bottom one to two kilometers of the hole is the waste emplacement zone where the nuclear canisters will be placed. The nuclear waste is encapsulated in casks in order to prevent corrosion and release of radioactivity into the surrounding ground water. Above the emplacement zone is the granite capstone region, typically greater than or equal to one kilometer thick. This region acts as a natural barrier between the surface and the entombed radionuclides. This barrier also prevents influence from the environment on the casks and the deep borehole system [1].

There are many motivations behind the very deep borehole concept. Because of the depth of the boreholes, the escape probability for radionuclides is low over a long time frame. As such, deep boreholes offer a high degree of protection from radionuclide exposure to people and the environment. Also, because of the many locations available for deep boreholes to be drilled, siting is facilitated. The natural and engineered barriers of the deep boreholes require little to no ongoing maintenance costs. Another benefit of the deep borehole concept is the reduced risk of proliferation. All of these reasons make the deep borehole concept an attractive method to store high level nuclear waste. Figure 1-1 shows the reference borehole concept.



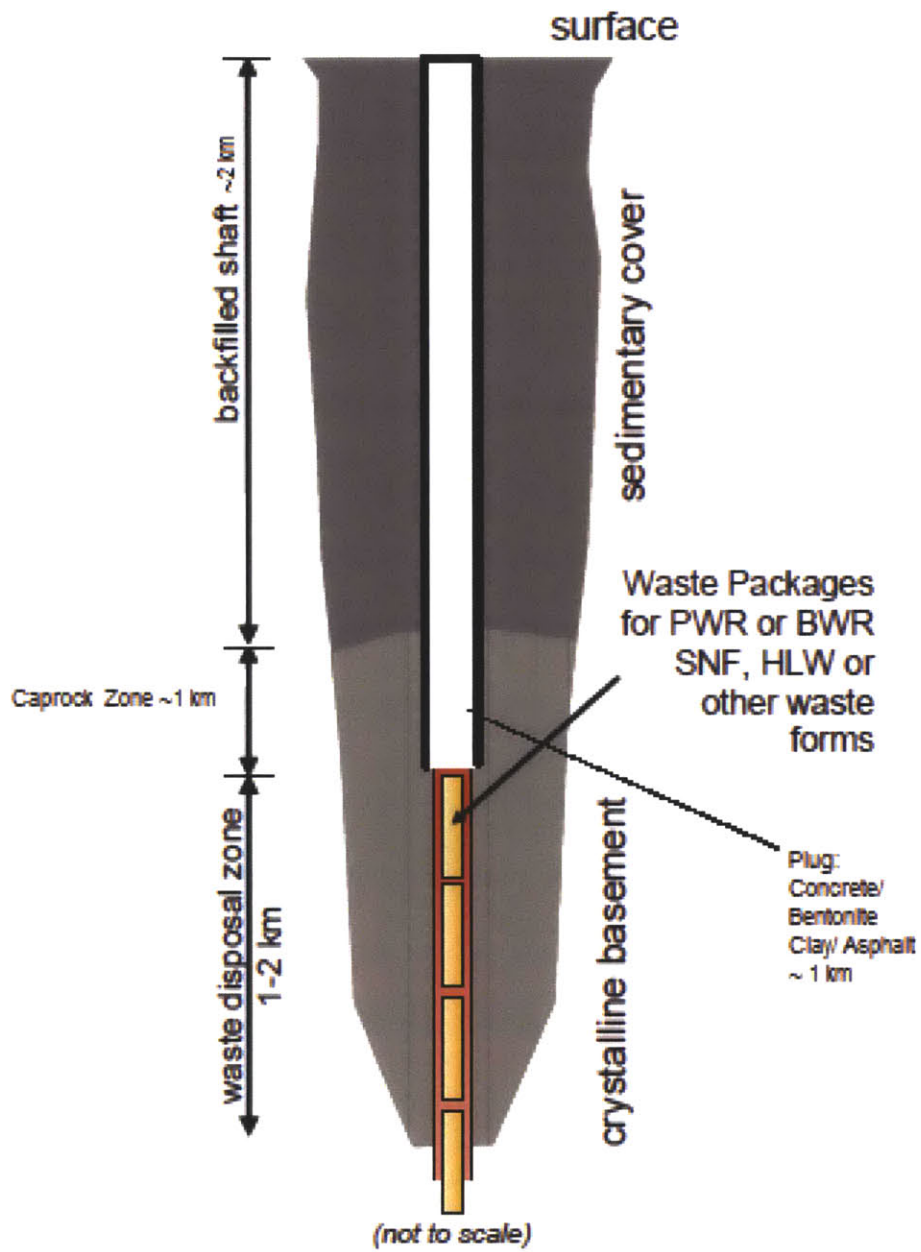


Figure 1-1 Deep Borehole Disposal Schematic [2]

## 1.2 Decay and Hazards of Nuclear Waste

Radiation can have harmful effects on biological organisms and the environment. Radiation can ionize particles and in the process damage the structure of biological molecules. Therefore, nuclear waste that contaminates the water supply can be hazardous to the local environment. As a result, the safe storage of nuclear waste is vital to any nuclear energy related field. One of the biggest factors affecting the safe storage of nuclear waste is the long lifetime of the radionuclides, which is on the order of tens of thousands of years and some even as long as, or longer than, a million years, e.g. Iodine-129 with a half-life of 16 million years. As such, nuclear waste fuel disposal facilities must be constructed to last for a very long time and must be able to withstand natural disasters that may influence it.

The nuclear waste generated from nuclear reactors is made up of fission products and minor actinides. Because the fission products are the result of the fission of very heavy atoms, which have many more neutrons than protons, these fission products tend to be very radioactive. The actinides are the result of neutron capture followed by beta decay, mostly starting with U-238, or alpha decay. These radionuclides produce a significant amount of heat and must be stored in such a way that this heat not only does not adversely affect the host environment, but that the heat does not cause the nuclear waste to melt, or otherwise leak and undergo accelerated dissolution in ambient water

### **1.3 Buoyancy Driven Nuclide Flow**

Over time, radionuclides will naturally leak out of the corroded casks. Because of the decay heat produced by the radionuclides, it is conceivable that the decay heat will create a significant temperature gradient within and close to the boreholes. As a result of the temperature gradient, a plume effect may be created which could cause the radionuclides in the water to rise over time and possibly escape from the borehole at its surface.

There are several conditions within the borehole that will affect how the radionuclides will travel. The density of the water will determine how fast the water will travel in the borehole. However, density changes as a function of temperature, pressure, and salinity. While it is almost impossible to vary the temperature and pressure within the borehole, it is possible to tailor the salinity of the water to suit our needs. This can be done by the careful choice of the borehole location. The porosity of the surrounding bedrock will also determine the diffusion rate of radionuclides through the cap rock. Potentially, at large distances underground away from the boreholes, the far field effects could potentially affect how the water will travel. The energy released by the decay of the radionuclides is the driving force behind the entire radionuclide movement. Figure 1-2 shows the thermal power released over time for commercial nuclear waste from a pressurized water reactor (PWR). As can be seen, after a century, the decay heat will

decrease by an order of magnitude, and after a thousand years fall to levels which are far less likely to promote both corrosive release and buoyancy-induced upflow.

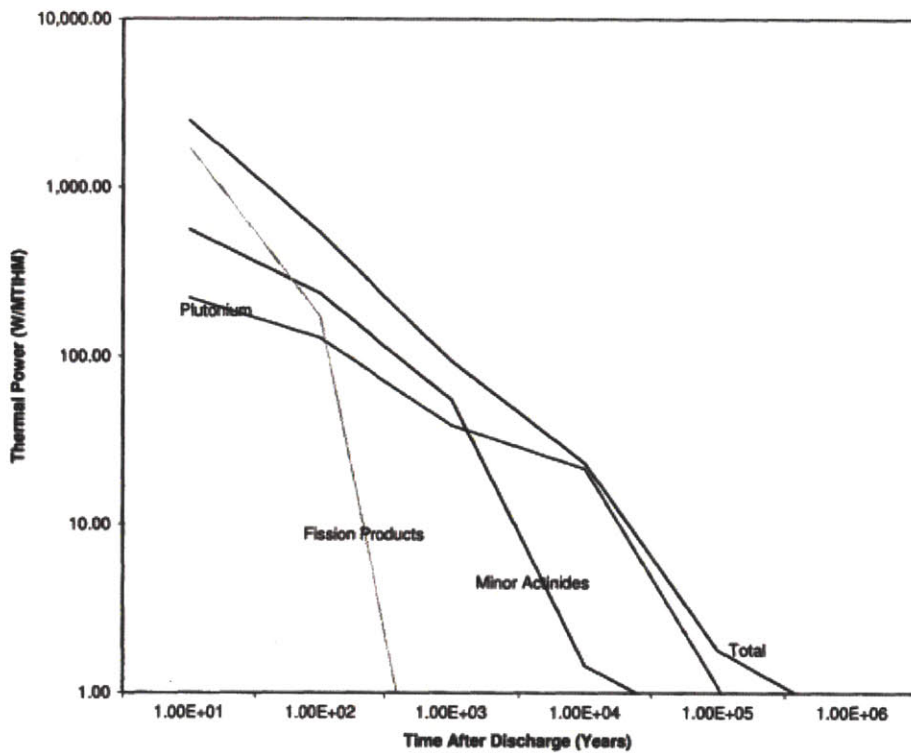


Figure 1-2 Log-Scale Thermal Power Released for Waste from a PWR for 1 MTIHM, 60,000 MWD/MTHM Burnup, and 10 Year Cooling [3]

## **2 Background Information**

### **2.1 Introduction**

While very deep boreholes offer significant protection against escape of radionuclides, due to their inherent geophysical and geochemical properties, their performance assurance relies on chemical and thermal-hydraulic modeling. Essentially the only escape mechanism is by transport of dissolved chemical species in water, as reviewed in this chapter.

### **2.2 Waterborne Radionuclide Transport**

Because of the very long half lives of some of the radionuclides that are the result of neutron irradiation, it is important to know the movements of the radionuclides for several thousand years after the casks have been placed. Because of cask fracture by corrosion, over the course of a few thousand years, the ambient water surrounding the casks could have a certain concentration of radionuclides. One of the main factors in

determining how fast the radionuclides will travel and thus escape is the host rock permeability. Equation 2-1 describes the velocity of the water as a function of the pressure gradient and time [4].

$$\frac{k}{\eta R} = \left( \frac{H\epsilon}{t} \right) \left( \frac{dP}{dz} \right)^{-1} \quad (2-1)$$

In Equation 2-1, k is the permeability in Darcys,

$$1 \text{ Darcy} = 0.97 \times 10^{-12} \text{ m}^2$$

$\eta$  is the dynamic viscosity of the fluid in centipoises, one centipoises is  $10^{-3}$  kg/(ms), R is the retardation factor due to sorption, H is the caprock thickness in centimeters,  $\epsilon$  is the rock porosity, t is the transit time in seconds, and  $\frac{dP}{dz}$  is the pressure gradient in bar per centimeter. From this equation, the expected hold up time can be calculated. For water at 55°C,  $\eta$  is 0.5 centipoise.

Similarly, Darcy's Law expressed in equation 2-2 describes the bulk projected velocity of water in a porous medium with a hydraulic gradient [1].

$$v = \left( \frac{k}{\eta} \right) \left( \frac{\Delta P}{\Delta z} \right) \quad (2-2)$$

Expressing Equation 2-2 as a function of density, the equation becomes

$$K = k \frac{g\rho}{\eta} \quad (2-3)$$

where  $K$  is the transit velocity in meters per second,  $g$  is the acceleration due to gravity  $9.81 \text{ m/s}^2$ , and  $\rho$  is the density in kilograms per cubic meter.

From equation 2-2 and 2-3, the escape fraction of the radionuclides in transit can be estimated. The escape fraction is defined as

$$EF = e^{-\lambda t} \quad (2-4)$$

where  $EF$  is the escape fraction,  $\lambda$  is the decay constant, and  $t$  is the time spent in transit.

### **2.3 Effects on Radionuclide Transport**

Different conditions affect the rate at which radionuclides will move through the bedrock. Since the salinity (hence density) of the water increases with depth in most continental shield bedrock, the water will be virtually stagnant down hole. However, this stagnation can be affected by the thermal output due to the decay heat from the casks. Heating of in-hole and adjacent water can produce an upward buoyant force due to reduced water density.

As the heated water moves up the borehole, there is a possibility that due to the reduced salinity in the far field region, the water will diffuse horizontally away from the borehole. However, as it diffuses away from the borehole, it will cool down. This will negate the upward driving force of the water and it will begin to fall back down. By the time it reaches the down hole depth, it will tend to move towards the much warmer near field region and thus will create a flow between the near field region and the far field region [5].

Another influence on the movement of the radionuclides is the water's movement in the caprock region. While the water is in the emplacement zone, it will have a constant heat source and thus will have a driving force allowing it to move up. However, after it leaves the emplacement zone, the only heat source it has is the radionuclides being carried along in the water. As a result, it is possible that the water will lose its driving force and will thus stagnate. As it stagnates, it will disperse its heat radially away from the borehole [5].

## **2.4 Plume Effect**

As noted, the water surrounding the casks can experience local heating. Because water density decreases with temperature increase, when there is localized heating, the density of the water will decrease. As a result, the heated water will rise, carrying the



radionuclides with it. While the density will slightly increase with depth due to the hydrostatic and lithostatic pressures exerted on the water, the density decrease due to a rise in temperature is much larger [1].

While the water is rising through the rocks, it must pass through the pores in the colder bedrock. As a result, in order for the water to continue to rise through the bedrock, the heating due to the radionuclides must offset the heat loss due to the heat transfer between the bedrock and the water. If the heat generated due to the radionuclide decay is less than the heat loss due to the heat transfer, then eventually the water's driving force will disappear and the water will stagnate. However, if the heat generated is greater than the heat loss, then the water should continue rising and eventually will penetrate the bedrock [1].

The overall conclusion is that a sufficient vertical salinity gradient can prevent initiation of this complicated water (hence radionuclide) circulation pattern. Hence the principal focus of this thesis is on quantification of the density vs. salinity relation for salts dissolved in water.

## **3 Density Calculations**

### **3.1 Introduction**

Because of the significant dependence that radionuclide transport has on the density of the saline water, it is important to determine the relationship that the density of water has on differing temperatures, pressures, and salinities. The density of the water will determine how the water will move inside the borehole and the host rock. Lower density water will move upward, while higher density water will naturally move downward. This behavior is important in terms of whether net upward flow dominates.

### **3.2 Effect of Pressure and Temperature**

Deep in the borehole, the pressure and temperature are high and must be taken into account with regards to the density of the water. At the depths in question, the pressure exerted on the water due to the lithostatic and hydrostatic pressure is on the order of 100 to 250 atm per kilometer, respectively [1]. In general, the hydrostatic

pressure is most often prevalent. As a result, the boiling point of the water is quite elevated and the water remains in the liquid phase.

The dependence of the density of water on the external pressure exerted on it is rather small. Because water is nearly incompressible, it requires a very large pressure to be exerted on it in order for the density to increase. At a depth of 4 km underground, the density of water will increase by approximately 1.6 percent [1].

On the other hand, the dependence of the density of water on the temperature of the water is quite significant. As the temperature of water increases, it expands and becomes much less dense. While the density of water at fifty atmospheres and 20 degrees Celsius is about  $1000.44 \text{ kg/m}^3$ , at the same pressure and a temperature of 200 degrees Celsius, the density falls to  $867.26 \text{ kg/m}^3$  [6]. This difference is much greater than the difference in density due to pressure. The data representing the dependence of water on its pressure and temperature is displayed in Appendix A.

### 3.3 Previous Salinity Experiments

Because most of the sites where the boreholes are drilled are located at sites where water may eventually become present, it is important to know how changes in water salinity will affect the water density. When salt is dissolved in water, the volume changes slightly as a function of the amount of solute dissolved.

Due to the uncertainty in this change in density, many previous experiments have been performed. These experiments tested the relationship between salinity and density for various pressures and temperatures. Based on some experiments compiled in the American Institute of Physics' *Journal of Physical and Chemical Reference Data* [7], an empirical formula relating density as a function of temperature, pressure, and salinity was developed by me in Equation 3-1.

$$\rho(T, P, S) = \rho_0 + 0.0378S + 4 * 10^{-5}P - (2 * 10^{-6}T^2 + 2.25 * 10^{-4}T) \quad (3-1)$$

In Equation 3-1 ,  $\rho_0$  is the density at a known, reference value, S is the molality in molals, in which 1 molal is defined as one mole of solute per 1 kilogram solvent, P is the pressure in bars, and T is the temperature in degrees Celsius. The equation above has an error of less than half a percent for values of salinity of 2 molals or less, temperatures of 200 degrees Celsius or less, and pressures of 400 bar or less. Equation 3-1 assumes that the density follows a linear increase. However, when the temperature, pressure, and/or the

salinity values increase beyond the values listed above, the rate of change in density begins to drop and thus Equation 3-1 will provide a result slightly larger than the actual value. Since the most significant factor affecting the density is the temperature, as the temperature increases, the rate of change in density increase begins to drop because the temperature of the water is approaching saturation. As a result, the water cannot continue to expand and eventually begins to vaporize. Figure 3-1 shows how density changes as a function of salinity for a few different temperatures and pressures.

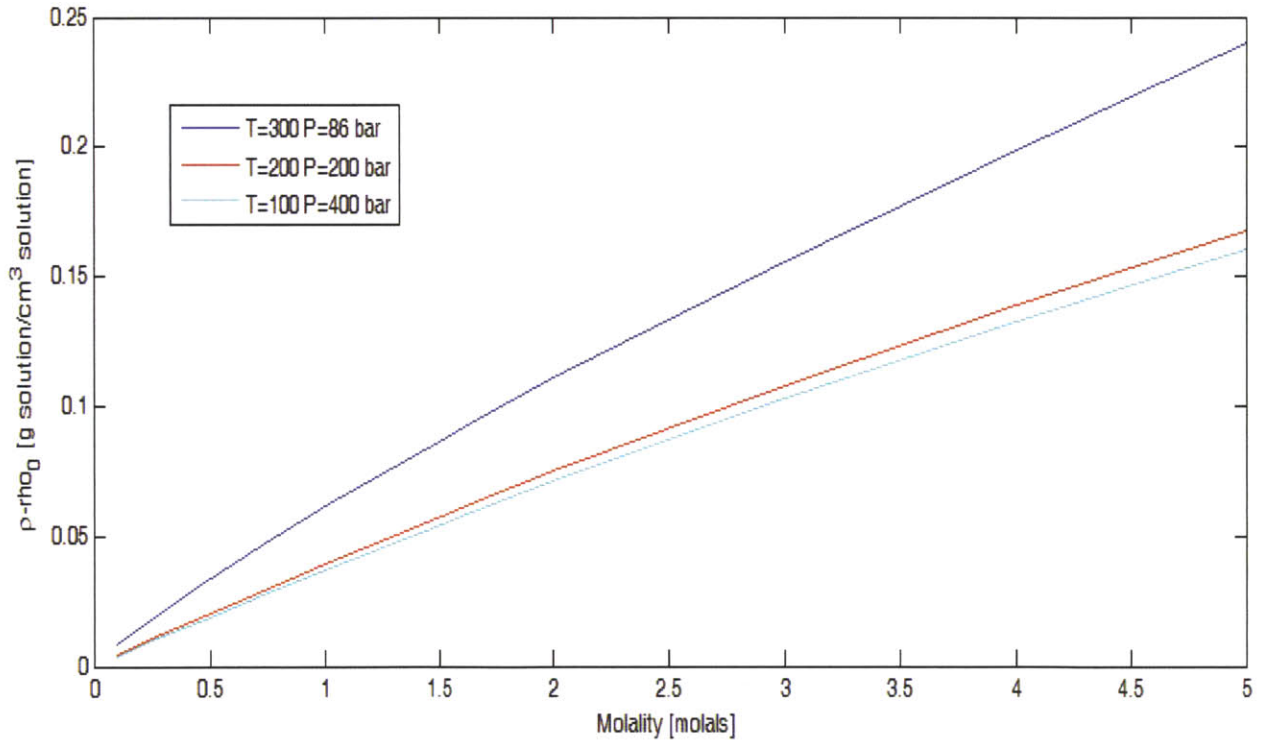


Figure 3-1 Change in water density as a function of salinity for three different temperatures and pressures.

Appendix B is a compilation of tables describing the relationship between specific volume and salinity for varying temperatures and pressures, in which specific volume is the inverse of the density.

### **3.4 Salinity vs. Density Experiments**

Because the water that will be used in deep boreholes may contain dissolved salts, it is important to know the relationship between density and salinity. However, it is uncertain whether or not different salts will act similarly. For instance, will sodium chloride (NaCl) act the same as calcium chloride (CaCl<sub>2</sub>)? The reason why sodium chloride may not act the same as calcium chloride is because of the extra ion in calcium chloride.

In order to test this, an experiment was designed. A one liter volumetric flask (see Figure 3-2) was filled with distilled water at room temperature. Afterwards, the salt being dissolved in the water (the first experiment involving sodium chloride at 98% purity, the second involving anhydrous calcium chloride at 96% purity) is measured out to known quantities, 0.1 mols, 0.25 mols, 0.5 mols, and finally 1.0 mols, and weighed on a balance. In incrementing steps, each quantity of salt was dissolved into the water. After having

sufficient time to fully dissolve into the water, first the change in height along the stem of the volumetric flask was measured, then using the Cole-Palmer Low-Cost Specific Gravity Meter, 1.000 to 1.300 SGU, °C model as seen in Figure 3-3, the density was again measured.

Because the volume of the flask, the mass of the water, the mass of the salt dissolved, and the change in height of the flask due to the salt, the change in volume of the flask and thus the change in density of the water can be calculated. This was done to confirm the accuracy of the density probe. Figure 3-4 shows the density as a function of molality for three different test runs, one sodium chloride trial and two calcium chloride trials, and Figure 3-5 shows the density as a function of mass dissolved salt per 1 kilogram water.

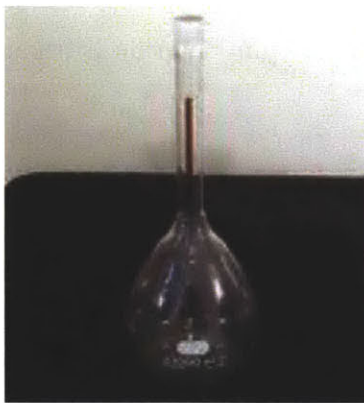


Figure 3-2 One liter Pyrex Volumetric Flask



Figure 3-3 Cole-Palmer Low-Cost Specific Gravity Meter, 1.000 to 1.300 SGU, °C  
model



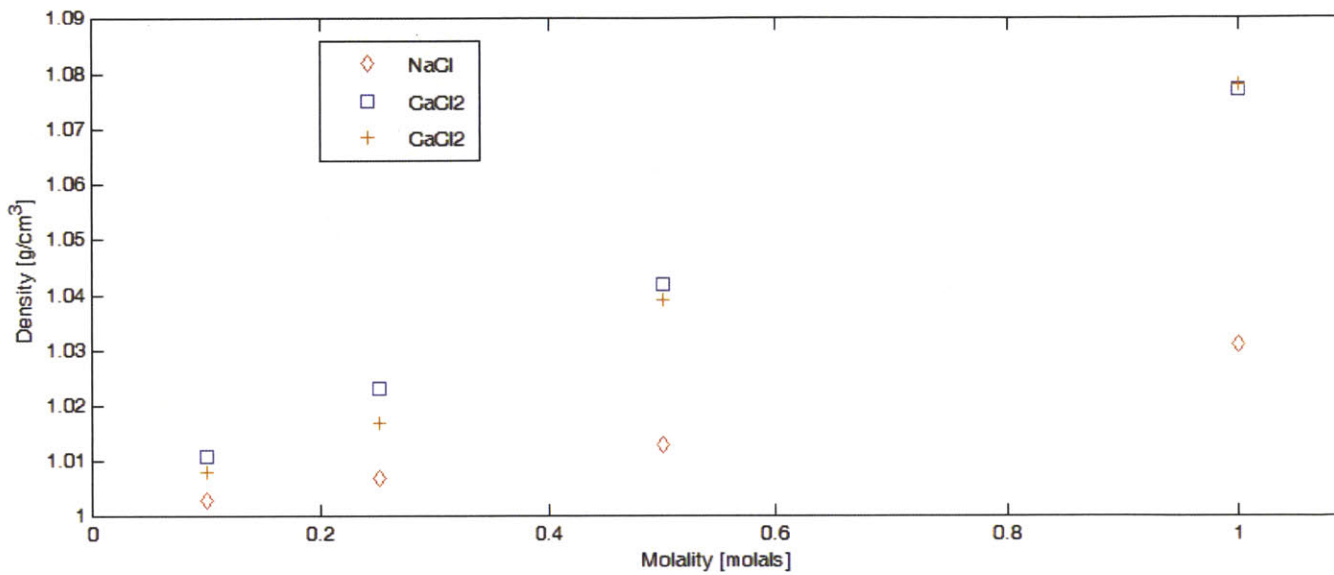


Figure 3-4 Density vs. Molality Results from Density Experiment Measured Using Density Probe

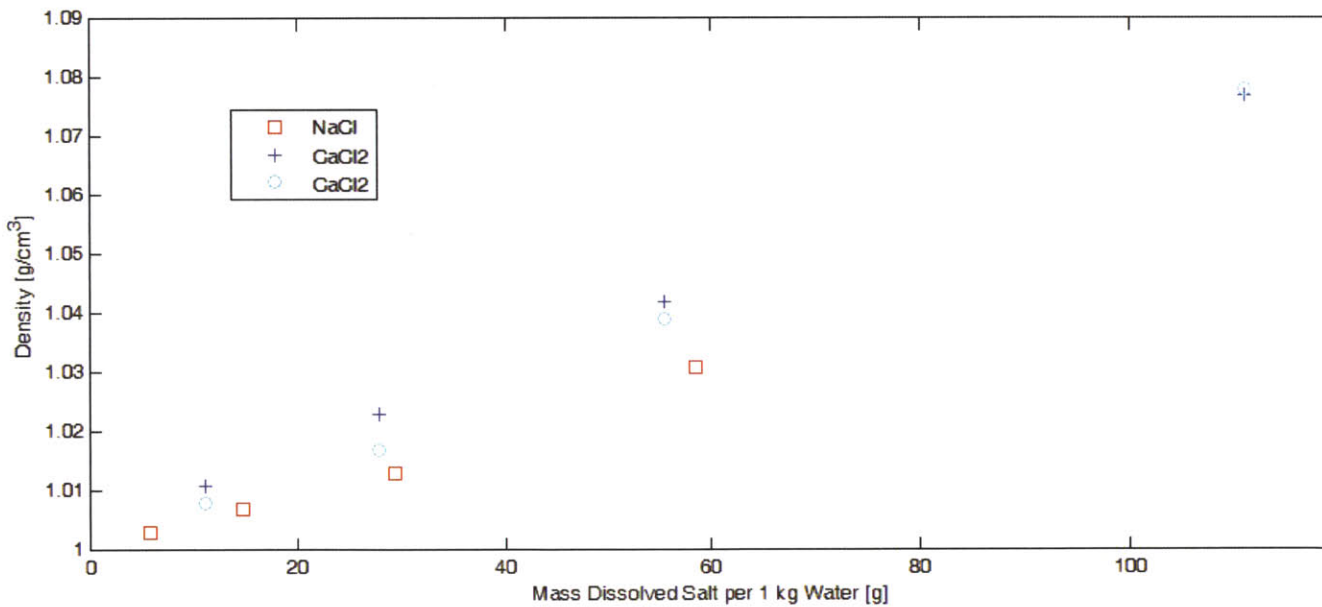


Figure 3-5 Density vs. Mass Ratio Results from Density Experiment Measured Using Density Probe

From the data collected, there is a clear relationship between the number of ions dissolved in the water and the density of the solution. The resulting relationship between the density of the water and the salinity is

$$\rho(S) = (0.02667 * n) * m + \rho_0 \quad (3-2)$$

where  $n$  is the number of ions being dissolved in the water,  $m$  is the molality, and  $\rho_0$  is the density with no solute dissolved at some reference temperature and pressure. For compounds like sodium chloride,  $n$  will be equal to two, while for calcium chloride,  $n$  will be three. For the relationship between density and the mass of the solute dissolved in water, the equation becomes

$$\rho(M) = (2.5 * 10^{-4} * n) * M + \rho_0 \quad (3-3)$$

where  $M$  is the mass of the salt dissolved in the water, and  $n$  is the number of ions of the compound. Based on the data from the CRC handbook relating salt dissolved in water and density, the data collected agreed within 1% of the literature values.

Some sources of error in the experiment are the uncertainties involved in measuring the change in height of the flask, some of the salt not completely dissolving in the water or otherwise not making it into the flask when the salt was added, air bubbles dissolved within the water, the impurities in the calcium chloride and sodium chloride salts, and the temperature of the water. Furthermore, when the calcium chloride was dissolving in the water, at times clumps of salt would form in the flask neck. Due to the effect of the heat of solution, the local temperature was measured to increase due to the

heat of solution for calcium chloride, which is  $-737.221 \text{ J/g}$ [8][9]. This may have resulted in some slight error in the density calculations, although some subsequent time was allowed for temperature equilibration and the meter corrects for water temperature.

## **4 Analysis**

### **4.1 Introduction**

Based on the information that has been collected thus far, it is important to determine how likely it is for radionuclides to escape from the borehole. Based on well known equations describing the movement of water through a porous medium, the velocity of the water through the bedrock and thus time it will take the radionuclides to escape from the borehole can be estimated.

### **4.2 Radionuclide Movement Timescale**

Under dry conditions, the movement of radionuclides in deep boreholes by means of diffusion is on such a long time scale that escape prior to decay is negligible [1]. Therefore, radionuclide escape due to water movement is the only viable method that

radionuclides could conceivably escape from the boreholes. From equation 2-3, the velocity of water through the host rock, given a porosity of  $10^{-5}$  Darcy is approximately  $1.9 \times 10^{-10}$  m/s. This yields an escape time of approximately  $10^5$  years. However, the porosity of  $10^{-5}$  Darcy is a rather conservative estimate and could well be a lower value. Also, there is retardation due to absorption by the rock surfaces. On the other hand, the density used for this calculation was assuming pure water, and thus the actual velocity assuming all other factors remain constant would be slightly higher. Nevertheless, this does give a good, conservative estimate on the escape timescale of radionuclides from the boreholes. However, the porosity of granite ranges from  $10^{-5}$  Darcys to  $10^{-9}$  Darcys [1]. Using the other end of the spectrum, the water velocity due to a porosity of  $10^{-9}$  Darcys is approximately  $1.9 \times 10^{-14}$  m/s yielding an escape time of about  $10^9$  years [1]. Note that these escape times are for radionuclides travelling through one kilometer of granite and thus do not take into account the top one kilometer of sedimentary rock. Because of the uncertainty in the porosity of the sedimentary rock, it is extremely difficult to model it accurately. Moreover the porosity is typically much higher-- e.g. several Darcy—and here transit time is much faster.

### 4.3 Radionuclide Escape Probability

Now that the water velocity is known and thus the radionuclide escape time, the escape probability of the radionuclides must be calculated. By the time that the radionuclides reach the surface based on the escape times, most of the radionuclides will have decayed away and the main contributor to the radionuclides will be neptunium-237 and/or Iodine-129. By using equation 2-4, which takes into account the decay rate of Iodine-129, the escape fraction for the radionuclides can be calculated.

For Iodine-129, the decay constant is approximately  $4.41 \times 10^{-8} \text{ yr}^{-1}$ . From this value and using the escape time for the conservative estimate, the escape fraction after  $10^5$  years is approximately 0.996. However, this value is more than likely a large overestimate of the actual escape value. Table 4-1 shows the escape fraction for varying levels of porosity.

**Table 4-1 Escape Fraction of Iodine-129 by Water Transport**

Porosity (k, Darcy)	Time (Years)	Escape Fraction
$10^{-5}$	$10^5$	0.996
$10^{-6}$	$10^6$	0.957
$10^{-7}$	$10^7$	0.643
$10^{-8}$	$10^8$	0.012
$10^{-9}$	$10^9$	$7.04 \times 10^{-20}$

As is seen in Table 4-1, the amount of radionuclides that escape from the borehole is progressively less as the porosity decreases. And since the porosity is smaller at large depths, the more likely average porosity would be closer to a value of  $10^{-7}$  Darcy or even smaller. Figure 4-1 shows the relationship between escape time and escape fraction up to a time of  $10^8$  years. Beyond that point it becomes almost impossible to distinguish the value of the escape fraction [1].

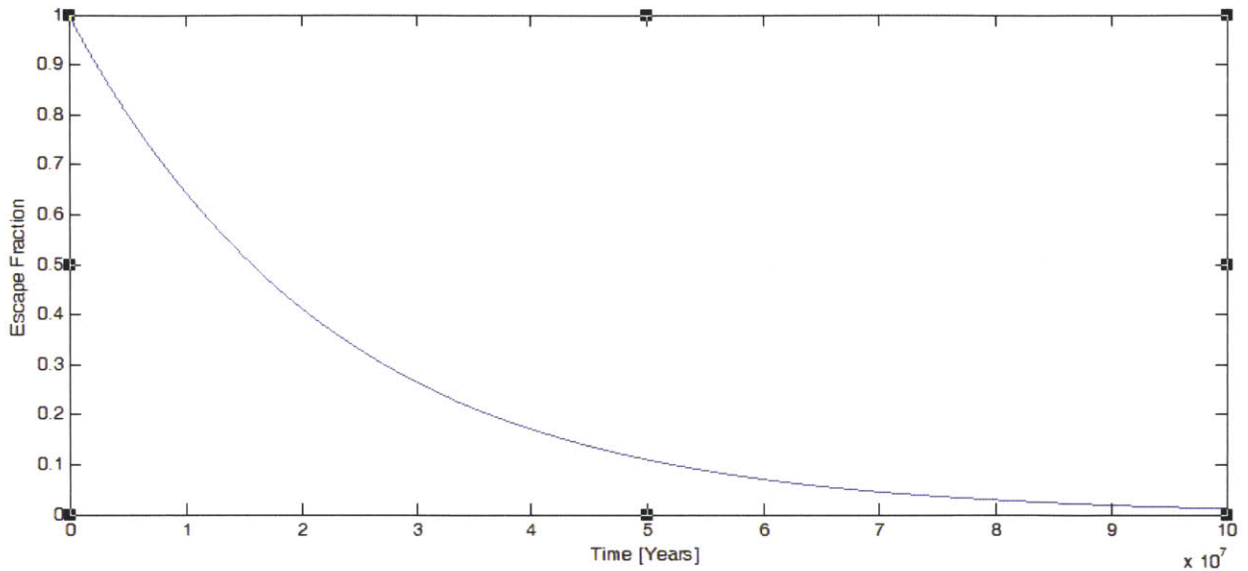


Figure 4-1 Escape fraction of Iodine-129 as a function of time.

Although it will take a porosity of less than  $5 \times 10^{-7}$  Darcy in order to achieve an escape time of fifty million years or greater, this is not an unreasonable value for the porosity of the host rock. As such, the danger that the radionuclides pose to people or the environment is minimal.

#### 4.4 Summary

While for quite porous rock of  $10^{-5}$  Darcy there is a significant amount of Iodine-129 that could escape, most of the host rocks used for deep boreholes will have a much lower porosity, due to the lithostatic pressure exerted on the rocks as well as the smaller



porosity of the host rock. Moreover, species such as iodine will be significantly retarded by absorption on such rock surfaces. In a more realistic scenario, it will take closer to five to ten million years for any radionuclides to escape from the borehole and even then, the amount that will escape will not have any significant affect.

## **5 Summary, Conclusions, and Recommendations**

### **5.1 Summary and Conclusions**

The very deep borehole concept offers a safe and viable method to store high level nuclear waste for a long time. The storage of nuclear waste in boreholes can offer protection for hundreds of thousands and perhaps millions of years. One concern about deep boreholes is the heat generated due to the nuclear decay causing localized heating. As a result of the heating, ambient water density will decrease and the resulting buoyancy-induced upflow could accelerate the time scale over which the radionuclides could potentially escape.

While initially the borehole would be placed in a dry location, the chance that flooding could occur is a possibility. Based on relationships describing the motion of water through a porous medium under hydrostatic pressure, the rate at which water would traverse the boreholes was calculated. In the most conservative estimate, it was found that it would take on the order of  $10^5$  years for the water to escape. However, this was very conservative and the actual timescale would probably be much greater. Factors influencing this would be the porosity of the host rock, its absorptive properties, the density of the water, the decay heat transferred into the water, and the salinity of the water.

As a result, the escape fraction of radionuclides from the borehole, which would be dominated by Neptunium-237 in an oxidizing environment, would be relatively small. A host rock having a porosity between  $10^{-6}$  Darcy and  $10^{-7}$  Darcy would reduce the escape fraction significantly and thus effectively completely contain the radionuclides.

Therefore, the deep borehole concept appears to be a viable option to store high level nuclear waste for a long period of time. While deep boreholes can store nuclear waste in the form of spent nuclear fuel, the available nuclear materials in dry storage could instead be used in a reprocessing facility, not only producing more energy, but at the same time producing more fuel to be used. The reprocessing of nuclear materials would reduce the amount of nuclear waste that would need to be stored in deep boreholes, and thus all that would be needed to be stored would be the dangerous fission products as well as the actinides that cannot be reprocessed.

## **5.2 Future Work**

There is still much research that needs to be performed on this concept. For example, a viable means of determining the best drill locations so that there are no anomalies when the boreholes are created is a necessity. Also, this thesis deals with a rough, simplistic model of the deep borehole concept. A more sophisticated, detailed simulation could produce much more accurate results and could determine problems that

would otherwise be neglected or completely missed. More research could be done on the porosities of granite which is generally dominated by interlinked microcracks, if different layers in the crust have different porosity spectrum, or what dependence pressure has on the host rock porosity.

## APPENDIX A: Steam Tables –From Ref. 10–

$t$ (°C)	$P$ bar	$\rho_l$ kg/m <sup>3</sup>	$\rho_g$ kg/m <sup>3</sup>	$h_f$ kJ/kg	$h_g$ kJ/kg	$\Delta h_{fg}$ kJ/kg	$s_f$ kJ/kg-K	$s_g$ kJ/kg-K	$\Delta s_{fg}$ kJ/kg-K	$v_f$ (m <sup>3</sup> /kg $\times 10^3$ )	$v_g$ (m <sup>3</sup> /kg $\times 10^3$ )
0.01	0.0061173	999.78	0.004855	0.00	2500.5	2500.5	0.00000	9.1541	9.1541	1.00022	205990
1	0.0065716	999.85	0.005196	4.18	2502.4	2498.2	0.01528	9.1277	9.1124	1.00015	192440
2	0.0070605	999.90	0.005563	8.40	2504.2	2495.8	0.03064	9.1013	9.0707	1.00010	179760
3	0.0075813	999.93	0.005952	12.61	2506.0	2493.4	0.04592	9.0752	9.0292	1.00007	168020
4	0.0081359	999.95	0.006364	16.82	2507.9	2491.1	0.06112	9.0492	8.9881	1.00005	157130
5	0.0087260	999.94	0.006802	21.02	2509.7	2488.7	0.07626	9.0236	8.9473	1.00006	147020
6	0.0093537	999.92	0.007265	25.22	2511.5	2486.3	0.09133	8.9981	8.9068	1.00008	137650
7	0.0100209	999.89	0.007756	29.42	2513.4	2484.0	0.10633	8.9729	8.8666	1.00011	128940
8	0.0107297	999.84	0.008275	33.61	2515.2	2481.6	0.12127	8.9479	8.8266	1.00016	120850
9	0.0114825	999.77	0.008824	37.80	2517.1	2479.3	0.13615	8.9232	8.7870	1.00023	113320
10	0.012281	999.69	0.009405	41.99	2518.9	2476.9	0.15097	8.8986	8.7477	1.00031	106320
11	0.013129	999.60	0.010019	46.18	2520.7	2474.5	0.16573	8.8743	8.7086	1.00040	99810
12	0.014027	999.49	0.010668	50.36	2522.6	2472.2	0.18044	8.8502	8.6698	1.00051	93740
13	0.014979	999.37	0.011353	54.55	2524.4	2469.8	0.19509	8.8263	8.6313	1.00063	88090
14	0.015988	999.24	0.012075	58.73	2526.2	2467.5	0.20969	8.8027	8.5930	1.00076	82810
15	0.017056	999.09	0.012837	62.92	2528.0	2465.1	0.22424	8.7792	8.5550	1.00091	77900
16	0.018185	998.93	0.013641	67.10	2529.9	2462.8	0.23873	8.7560	8.5173	1.00107	73310
17	0.019380	998.76	0.014488	71.28	2531.7	2460.4	0.25317	8.7330	8.4798	1.00124	69020
18	0.020644	998.58	0.015380	75.47	2533.5	2458.1	0.26757	8.7101	8.4426	1.00142	65020
19	0.021979	998.39	0.016319	79.65	2535.3	2455.7	0.28191	8.6875	8.4056	1.00161	61280
20	0.023388	998.19	0.017308	83.84	2537.2	2453.3	0.29621	8.6651	8.3689	1.00182	57778
21	0.024877	997.97	0.018347	88.02	2539.0	2451.0	0.31045	8.6428	8.3324	1.00203	54503
22	0.026447	997.75	0.019441	92.20	2540.8	2448.6	0.32465	8.6208	8.2962	1.00226	51438
23	0.028104	997.52	0.020590	96.39	2542.6	2446.2	0.33880	8.5990	8.2602	1.00249	48568
24	0.029850	997.27	0.021797	100.57	2544.5	2443.9	0.35290	8.5773	8.2244	1.00274	45878
25	0.031691	997.02	0.023065	104.75	2546.3	2441.5	0.36696	8.5558	8.1889	1.00299	43357
26	0.033629	996.75	0.024395	108.94	2548.1	2439.2	0.38096	8.5346	8.1536	1.00326	40992
27	0.035670	996.48	0.025791	113.12	2549.9	2436.8	0.39492	8.5135	8.1185	1.00353	38773
28	0.037818	996.20	0.027255	117.30	2551.7	2434.4	0.40884	8.4926	8.0837	1.00381	36690
29	0.040078	995.91	0.028791	121.49	2553.5	2432.0	0.42271	8.4718	8.0491	1.00411	34734
30	0.042455	995.61	0.030399	125.67	2555.3	2429.7	0.43653	8.4513	8.0147	1.00441	32896
31	0.044953	995.30	0.032084	129.85	2557.1	2427.3	0.45031	8.4309	7.9806	1.00472	31168
32	0.047578	994.99	0.033849	134.04	2559.0	2424.9	0.46404	8.4107	7.9466	1.00504	29543
33	0.050335	994.66	0.035696	138.22	2560.8	2422.5	0.47772	8.3906	7.9129	1.00537	28014
34	0.053229	994.33	0.037629	142.40	2562.6	2420.2	0.49137	8.3708	7.8794	1.00570	26575
35	0.056267	993.99	0.039650	146.59	2564.4	2417.8	0.50496	8.3511	7.8461	1.00605	25220
36	0.059454	993.64	0.041764	150.77	2566.2	2415.4	0.51851	8.3315	7.8130	1.00640	23944
37	0.062795	993.28	0.043973	154.95	2568.0	2413.0	0.53202	8.3122	7.7802	1.00676	22741
38	0.066298	992.92	0.046281	159.14	2569.8	2410.6	0.54549	8.2930	7.7475	1.00713	21607
39	0.069969	992.55	0.048691	163.32	2571.6	2408.2	0.55891	8.2739	7.7150	1.00751	20538
40	0.073814	992.17	0.05121	167.50	2573.4	2405.9	0.57228	8.2550	7.6828	1.00789	19528
41	0.077840	991.78	0.05383	171.69	2575.2	2403.5	0.58562	8.2363	7.6507	1.00829	18576
42	0.082054	991.39	0.05657	175.87	2576.9	2401.1	0.59891	8.2177	7.6188	1.00869	17676
43	0.086464	990.99	0.05943	180.05	2578.7	2398.7	0.61216	8.1993	7.5872	1.00909	16826
44	0.091076	990.58	0.06241	184.23	2580.5	2396.3	0.62537	8.1810	7.5557	1.00951	16023
45	0.095898	990.17	0.06552	188.42	2582.3	2393.9	0.63853	8.1629	7.5244	1.00993	15263
46	0.100938	989.74	0.06875	192.60	2584.1	2391.5	0.65166	8.1450	7.4933	1.01036	14545
47	0.106205	989.32	0.07212	196.78	2585.9	2389.1	0.66474	8.1271	7.4624	1.01080	13866
48	0.111706	988.88	0.07563	200.96	2587.6	2386.7	0.67778	8.1094	7.4317	1.01124	13222
49	0.117449	988.44	0.07928	205.14	2589.4	2384.3	0.69078	8.0919	7.4011	1.01170	12614
50	0.12344	987.99	0.08308	209.33	2591.2	2381.9	0.70374	8.0745	7.3708	1.01215	12037
51	0.12970	987.54	0.08703	213.51	2593.0	2379.5	0.71666	8.0573	7.3406	1.01262	11490
52	0.13623	987.08	0.09114	217.69	2594.7	2377.0	0.72954	8.0401	7.3106	1.01309	10972
53	0.14303	986.61	0.09541	221.87	2596.5	2374.6	0.74238	8.0232	7.2808	1.01357	10481
54	0.15012	986.13	0.09985	226.06	2598.3	2372.2	0.75518	8.0063	7.2511	1.01406	10015

$t(^{\circ}\text{C})$	$P$ bar	$\rho_l$ kg/m <sup>3</sup>	$\rho_g$ kg/m <sup>3</sup>	$h_f$ kJ/kg	$h_g$ kJ/kg	$\Delta h_g$ kJ/kg	$s_l$ kJ/kg-K	$s_g$ kJ/kg-K	$\Delta s_g$ kJ/kg-K	$v_f$ (m <sup>3</sup> /kg $\times 10^3$ )	$v_g$ (m <sup>3</sup> /kg $\times 10^3$ )
55	0.15752	985.65	0.10446	230.24	2600.0	2369.8	0.76795	7.9896	7.2216	1.01455	9573.
56	0.16522	985.17	0.10925	234.42	2601.8	2367.4	0.78067	7.9730	7.1923	1.01505	9153.
57	0.17324	984.68	0.11423	238.60	2603.5	2364.9	0.79336	7.9566	7.1632	1.01556	8754.
58	0.18159	984.18	0.11939	242.79	2605.3	2362.5	0.80600	7.9402	7.1342	1.01608	8376.
59	0.19028	983.67	0.12475	246.97	2607.0	2360.1	0.81862	7.9240	7.1054	1.01660	8016.
60	0.19932	983.16	0.13030	251.15	2608.8	2357.6	0.83119	7.9080	7.0768	1.01712	7674.
61	0.20873	982.65	0.13607	255.34	2610.5	2355.2	0.84373	7.8920	7.0483	1.01766	7349.
62	0.21851	982.13	0.14204	259.52	2612.3	2352.8	0.85622	7.8762	7.0200	1.01820	7040.
63	0.22868	981.60	0.14824	263.71	2614.0	2350.3	0.86869	7.8605	6.9918	1.01875	6746.
64	0.23925	981.07	0.15465	267.89	2615.8	2347.9	0.88112	7.8450	6.9638	1.01930	6466.
65	0.25022	980.53	0.16130	272.08	2617.5	2345.4	0.89351	7.8295	6.9360	1.01986	6200.
66	0.26163	979.98	0.16819	276.26	2619.2	2343.0	0.90586	7.8142	6.9083	1.02043	5946.
67	0.27347	979.43	0.17532	280.45	2620.9	2340.5	0.91819	7.7989	6.8808	1.02100	5704.
68	0.28576	978.88	0.18269	284.63	2622.7	2338.0	0.93047	7.7838	6.8534	1.02158	5474.
69	0.29852	978.32	0.19033	288.82	2624.4	2335.6	0.94272	7.7689	6.8261	1.02216	5254.
70	0.31176	977.75	0.19823	293.01	2626.1	2333.1	0.95494	7.7540	6.7990	1.02276	5044.6
71	0.32549	977.18	0.20640	297.20	2627.8	2330.6	0.96713	7.7392	6.7721	1.02336	4844.9
72	0.33972	976.60	0.21485	301.39	2629.5	2328.1	0.97928	7.7246	6.7453	1.02396	4654.4
73	0.35448	976.02	0.22358	305.58	2631.2	2325.7	0.99139	7.7100	6.7186	1.02457	4472.6
74	0.36978	975.43	0.23261	309.77	2632.9	2323.2	1.00348	7.6956	6.6921	1.02519	4299.0
75	0.38563	974.84	0.24194	313.96	2634.6	2320.7	1.01553	7.6813	6.6657	1.02581	4133.3
76	0.40205	974.24	0.25158	318.15	2636.3	2318.2	1.02754	7.6670	6.6395	1.02644	3975.0
77	0.41905	973.64	0.26153	322.34	2638.0	2315.7	1.03953	7.6529	6.6134	1.02708	3823.7
78	0.43665	973.03	0.27180	326.54	2639.7	2313.2	1.05149	7.6389	6.5874	1.02772	3679.1
79	0.45487	972.41	0.28241	330.73	2641.4	2310.7	1.06341	7.6250	6.5616	1.02837	3541.0
80	0.47373	971.79	0.29336	334.93	2643.1	2308.1	1.07530	7.6112	6.5359	1.02902	3408.8
81	0.49324	971.17	0.30465	339.12	2644.7	2305.6	1.08716	7.5975	6.5103	1.02969	3282.4
82	0.51342	970.54	0.31631	343.32	2646.4	2303.1	1.09899	7.5838	6.4849	1.03035	3161.5
83	0.53428	969.91	0.32832	347.52	2648.1	2300.6	1.11079	7.5703	6.4595	1.03103	3045.8
84	0.55585	969.27	0.34072	351.72	2649.7	2298.0	1.12255	7.5569	6.4344	1.03171	2935.0
85	0.57815	968.62	0.35349	355.92	2651.4	2295.5	1.13429	7.5436	6.4093	1.03239	2828.9
86	0.60119	967.98	0.36666	360.12	2653.1	2292.9	1.14600	7.5304	6.3844	1.03308	2727.3
87	0.62499	967.32	0.38023	364.32	2654.7	2290.4	1.15768	7.5172	6.3595	1.03378	2630.0
88	0.64958	966.66	0.39420	368.52	2656.4	2287.8	1.16932	7.5042	6.3349	1.03449	2536.8
89	0.67496	966.00	0.40860	372.73	2658.0	2285.3	1.18094	7.4912	6.3103	1.03520	2447.4
90	0.70117	965.33	0.42343	376.93	2659.6	2282.7	1.19253	7.4784	6.2858	1.03591	2361.7
91	0.72823	964.66	0.43870	381.14	2661.3	2280.1	1.20409	7.4656	6.2615	1.03664	2279.5
92	0.75614	963.98	0.45441	385.35	2662.9	2277.5	1.21563	7.4529	6.2373	1.03736	2200.7
93	0.78495	963.30	0.47058	389.56	2664.5	2275.0	1.22713	7.4403	6.2132	1.03810	2125.0
94	0.81465	962.61	0.48723	393.77	2666.1	2272.4	1.23861	7.4278	6.1892	1.03884	2052.4
95	0.84529	961.92	0.5043	397.98	2667.7	2269.8	1.25006	7.4154	6.1653	1.03959	1982.8
96	0.87688	961.22	0.5220	402.20	2669.4	2267.2	1.26148	7.4030	6.1416	1.04034	1915.9
97	0.90945	960.52	0.5401	406.41	2671.0	2264.5	1.27287	7.3908	6.1179	1.04110	1851.6
98	0.94301	959.82	0.5587	410.63	2672.5	2261.9	1.28424	7.3786	6.0944	1.04186	1789.9
99	0.97759	959.11	0.5778	414.84	2674.1	2259.3	1.29557	7.3665	6.0709	1.04264	1730.6
100	1.0132	958.39	0.5975	419.06	2675.7	2256.7	1.30689	7.3545	6.0476	1.04341	1673.6
101	1.0499	957.67	0.6177	423.28	2677.3	2254.0	1.31817	7.3426	6.0244	1.04420	1618.9
102	1.0877	956.95	0.6385	427.51	2678.9	2251.4	1.32943	7.3307	6.0013	1.04499	1566.2
103	1.1266	956.22	0.6598	431.73	2680.5	2248.7	1.34066	7.3189	5.9783	1.04578	1515.5
104	1.1667	955.49	0.6817	435.95	2682.0	2246.1	1.35187	7.3072	5.9553	1.04659	1466.8
105	1.2079	954.75	0.7042	440.18	2683.6	2243.4	1.36305	7.2956	5.9325	1.04739	1420.0
106	1.2503	954.01	0.7273	444.41	2685.1	2240.7	1.37420	7.2840	5.9098	1.04821	1374.9
107	1.2939	953.26	0.7511	448.64	2686.7	2238.0	1.38533	7.2726	5.8872	1.04903	1331.4
108	1.3388	952.51	0.7754	452.87	2688.2	2235.3	1.39644	7.2612	5.8647	1.04986	1289.6
109	1.3850	951.75	0.8004	457.10	2689.7	2232.6	1.40751	7.2498	5.8423	1.05069	1249.4

$t(^{\circ}\text{C})$	$P$ bar	$\rho_l$ kg/m <sup>3</sup>	$\rho_g$ kg/m <sup>3</sup>	$h_f$ kJ/kg	$h_g$ kJ/kg	$\Delta h_g$ kJ/kg	$s_f$ kJ/kg-K	$s_g$ kJ/kg-K	$\Delta S_{fg}$ kJ/kg-K	$v_f$ (m <sup>3</sup> /kg $\times 10^3$ )	$v_g$ (m <sup>3</sup> /kg $\times 10^3$ )
110	1.4324	951.00	0.8260	461.34	2691.3	2229.9	1.41857	7.2386	5.8200	1.05153	1210.6
111	1.4812	950.23	0.8523	465.57	2692.8	2227.2	1.42960	7.2274	5.7978	1.05238	1173.3
112	1.5313	949.46	0.8793	469.81	2694.3	2224.5	1.44060	7.2163	5.7757	1.05323	1137.3
113	1.5829	948.69	0.9069	474.05	2695.8	2221.8	1.45158	7.2052	5.7536	1.05409	1102.6
114	1.6358	947.91	0.9353	478.29	2697.3	2219.0	1.46253	7.1942	5.7317	1.05495	1069.2
115	1.6902	947.13	0.9643	482.54	2698.8	2216.3	1.47347	7.1833	5.7099	1.05582	1037.0
116	1.7461	946.34	0.9941	486.78	2700.3	2213.5	1.48437	7.1725	5.6881	1.05670	1005.9
117	1.8034	945.55	1.0247	491.03	2701.8	2210.8	1.49526	7.1617	5.6664	1.05758	975.9
118	1.8623	944.76	1.0559	495.28	2703.3	2208.0	1.50612	7.1510	5.6449	1.05847	947.0
119	1.9228	943.96	1.0880	499.53	2704.7	2205.2	1.51695	7.1403	5.6234	1.05937	919.1
120	1.9848	943.16	1.1208	503.78	2706.2	2202.4	1.52776	7.1297	5.6020	1.06027	892.2
121	2.0485	942.35	1.1545	508.03	2707.6	2199.6	1.53855	7.1192	5.5807	1.06118	866.2
122	2.1139	941.54	1.1889	512.29	2709.1	2196.8	1.54932	7.1087	5.5594	1.06210	841.1
123	2.1809	940.72	1.2242	516.55	2710.5	2194.0	1.56006	7.0983	5.5383	1.06302	816.9
124	2.2496	939.90	1.2603	520.81	2712.0	2191.2	1.57078	7.0880	5.5172	1.06395	793.5
125	2.3201	939.07	1.2972	525.07	2713.4	2188.3	1.58148	7.0777	5.4962	1.06488	770.9
126	2.3924	938.24	1.3351	529.33	2714.8	2185.5	1.59216	7.0675	5.4753	1.06582	749.0
127	2.4666	937.41	1.3738	533.60	2716.2	2182.6	1.60281	7.0573	5.4545	1.06677	727.9
128	2.5425	936.57	1.4134	537.86	2717.6	2179.8	1.61344	7.0472	5.4338	1.06772	707.5
129	2.6204	935.73	1.4539	542.13	2719.0	2176.9	1.62405	7.0372	5.4131	1.06869	687.8
130	2.7002	934.88	1.4954	546.41	2720.4	2174.0	1.63464	7.0272	5.3925	1.06965	668.7
131	2.7820	934.03	1.5378	550.68	2721.8	2171.1	1.64521	7.0172	5.3720	1.07063	650.3
132	2.8657	933.18	1.5811	554.96	2723.2	2168.2	1.65575	7.0074	5.3516	1.07161	632.5
133	2.9515	932.32	1.6255	559.23	2724.5	2165.3	1.66628	6.9975	5.3313	1.07260	615.2
134	3.0393	931.45	1.6708	563.52	2725.9	2162.4	1.67678	6.9878	5.3110	1.07359	598.5
135	3.1293	930.59	1.7172	567.80	2727.2	2159.4	1.68726	6.9780	5.2908	1.07459	582.4
136	3.2214	929.71	1.7646	572.08	2728.6	2156.5	1.69772	6.9684	5.2706	1.07560	566.7
137	3.3157	928.84	1.8130	576.37	2729.9	2153.5	1.70816	6.9587	5.2506	1.07661	551.6
138	3.4122	927.96	1.8625	580.66	2731.2	2150.6	1.71858	6.9492	5.2306	1.07764	536.9
139	3.5109	927.07	1.9130	584.95	2732.5	2147.6	1.72898	6.9397	5.2107	1.07866	522.7
140	3.6119	926.18	1.9647	589.24	2733.8	2144.6	1.73936	6.9302	5.1908	1.07970	508.99
141	3.7153	925.29	2.0174	593.54	2735.1	2141.6	1.74972	6.9208	5.1711	1.08074	495.68
142	3.8211	924.39	2.0713	597.84	2736.4	2138.6	1.76006	6.9114	5.1513	1.08179	482.78
143	3.9292	923.49	2.1264	602.14	2737.7	2135.6	1.77038	6.9021	5.1317	1.08285	470.28
144	4.0398	922.58	2.1826	606.44	2739.0	2132.5	1.78068	6.8928	5.1121	1.08391	458.17
145	4.1529	921.67	2.2400	610.75	2740.2	2129.5	1.79096	6.8836	5.0926	1.08498	446.43
146	4.2685	920.76	2.2986	615.06	2741.5	2126.4	1.80122	6.8744	5.0732	1.08606	435.05
147	4.3867	919.84	2.3584	619.37	2742.7	2123.3	1.81146	6.8652	5.0538	1.08715	424.01
148	4.5075	918.92	2.4195	623.68	2743.9	2120.3	1.82169	6.8562	5.0345	1.08824	413.31
149	4.6310	917.99	2.4818	628.00	2745.2	2117.2	1.83189	6.8471	5.0152	1.08934	402.93
150	4.7572	917.06	2.5454	632.32	2746.4	2114.1	1.84208	6.8381	4.9960	1.09044	392.86
151	4.8861	916.12	2.6104	636.64	2747.6	2110.9	1.85224	6.8291	4.9769	1.09156	383.09
152	5.0178	915.18	2.6766	640.96	2748.8	2107.8	1.86239	6.8202	4.9578	1.09268	373.61
153	5.1523	914.24	2.7442	645.29	2750.0	2104.7	1.87252	6.8113	4.9388	1.09381	364.41
154	5.2896	913.29	2.8131	649.62	2751.1	2101.5	1.88263	6.8025	4.9198	1.09495	355.48
155	5.4299	912.33	2.8834	653.95	2752.3	2098.3	1.89273	6.7937	4.9010	1.09609	346.81
156	5.5732	911.38	2.9551	658.28	2753.4	2095.2	1.90280	6.7849	4.8821	1.09724	338.40
157	5.7194	910.41	3.0282	662.62	2754.6	2092.0	1.91286	6.7762	4.8633	1.09840	330.23
158	5.8687	909.45	3.1028	666.96	2755.7	2088.8	1.92290	6.7675	4.8446	1.09957	322.29
159	6.0211	908.48	3.1788	671.30	2756.8	2085.5	1.93292	6.7589	4.8260	1.10074	314.58
160	6.1766	907.50	3.2564	675.65	2758.0	2082.3	1.94293	6.7503	4.8073	1.10193	307.09
161	6.3353	906.52	3.3354	680.00	2759.1	2079.1	1.95292	6.7417	4.7888	1.10312	299.82
162	6.4973	905.54	3.4159	684.35	2760.1	2075.8	1.96289	6.7332	4.7703	1.10432	292.75
163	6.6625	904.55	3.4980	688.71	2761.2	2072.5	1.97284	6.7247	4.7518	1.10552	285.87
164	6.8310	903.56	3.5817	693.07	2762.3	2069.2	1.98278	6.7162	4.7334	1.10674	279.19

$t$ (°C)	$P$ bar	$\rho_l$ kg/m <sup>3</sup>	$\rho_g$ kg/m <sup>3</sup>	$h_l$ kJ/kg	$h_g$ kJ/kg	$\Delta h_g$ kJ/kg	$s_l$ kJ/kg-K	$s_g$ kJ/kg-K	$\Delta S_g$ kJ/kg-K	$v_1$ (m <sup>3</sup> /kg ×10 <sup>3</sup> )	$v_g$ (m <sup>3</sup> /kg ×10 <sup>3</sup> )
165	7.0029	902.56	3.6670	697.43	2763.3	2065.9	1.99271	6.7078	4.7151	1.10796	272.70
166	7.1783	901.56	3.7539	701.79	2764.4	2062.6	2.00261	6.6994	4.6968	1.10919	266.39
167	7.3570	900.55	3.8424	706.16	2765.4	2059.3	2.01250	6.6910	4.6785	1.11043	260.25
168	7.5394	899.54	3.9326	710.53	2766.4	2055.9	2.02237	6.6827	4.6603	1.11168	254.28
169	7.7252	898.53	4.0245	714.90	2767.5	2052.5	2.03223	6.6744	4.6422	1.11293	248.48
170	7.9147	897.51	4.1181	719.28	2768.5	2049.2	2.04207	6.6662	4.6241	1.11420	242.83
171	8.1078	896.48	4.2135	723.66	2769.4	2045.8	2.05190	6.6579	4.6060	1.11547	237.33
172	8.3047	895.46	4.3106	728.05	2770.4	2042.4	2.06171	6.6498	4.5880	1.11675	231.99
173	8.5053	894.42	4.4095	732.43	2771.4	2038.9	2.07150	6.6416	4.5701	1.11804	226.78
174	8.7098	893.38	4.5102	736.83	2772.3	2035.5	2.08128	6.6335	4.5522	1.11934	221.72
175	8.9180	892.34	4.6127	741.22	2773.3	2032.0	2.09105	6.6254	4.5343	1.12065	216.79
176	9.1303	891.30	4.7172	745.62	2774.2	2028.6	2.10080	6.6173	4.5165	1.12196	211.99
177	9.3464	890.24	4.8235	750.02	2775.1	2025.1	2.11054	6.6092	4.4987	1.12329	207.32
178	9.5666	889.19	4.9317	754.43	2776.0	2021.6	2.12026	6.6012	4.4810	1.12462	202.77
179	9.7909	888.13	5.0418	758.84	2776.9	2018.1	2.12996	6.5932	4.4633	1.12596	198.34
180	10.019	887.06	5.154	763.25	2777.8	2014.5	2.13966	6.5853	4.4456	1.12732	194.03
181	10.252	885.99	5.268	767.67	2778.6	2011.0	2.14934	6.5774	4.4280	1.12868	189.82
182	10.489	884.92	5.384	772.09	2779.5	2007.4	2.15900	6.5694	4.4104	1.13005	185.73
183	10.730	883.84	5.502	776.51	2780.3	2003.8	2.16865	6.5616	4.3929	1.13143	181.74
184	10.975	882.75	5.623	780.94	2781.2	2000.2	2.17829	6.5537	4.3754	1.13282	177.85
185	11.225	881.67	5.745	785.37	2782.0	1996.6	2.18791	6.5459	4.3580	1.13422	174.06
186	11.479	880.57	5.870	789.81	2782.8	1993.0	2.19752	6.5381	4.3406	1.13563	170.37
187	11.738	879.47	5.996	794.25	2783.6	1989.3	2.20712	6.5303	4.3232	1.13704	166.77
188	12.001	878.37	6.125	798.69	2784.3	1985.6	2.21670	6.5226	4.3059	1.13847	163.26
189	12.269	877.26	6.256	803.14	2785.1	1982.0	2.22628	6.5148	4.2886	1.13991	159.84
190	12.542	876.15	6.390	807.60	2785.8	1978.2	2.23583	6.5071	4.2713	1.14136	156.50
191	12.819	875.03	6.525	812.06	2786.6	1974.5	2.24538	6.4994	4.2541	1.14282	153.25
192	13.101	873.91	6.663	816.52	2787.3	1970.8	2.25491	6.4918	4.2369	1.14429	150.08
193	13.388	872.78	6.804	820.98	2788.0	1967.0	2.26444	6.4841	4.2197	1.14576	146.98
194	13.680	871.65	6.946	825.46	2788.7	1963.2	2.27395	6.4765	4.2026	1.14725	143.96
195	13.976	870.51	7.091	829.93	2789.4	1959.4	2.28344	6.4689	4.1855	1.14875	141.02
196	14.278	869.37	7.239	834.41	2790.0	1955.6	2.29293	6.4613	4.1684	1.15026	138.14
197	14.585	868.22	7.389	838.90	2790.7	1951.8	2.30241	6.4538	4.1514	1.15178	135.34
198	14.897	867.07	7.541	843.39	2791.3	1947.9	2.31187	6.4463	4.1344	1.15332	132.60
199	15.214	865.91	7.697	847.88	2791.9	1944.0	2.32132	6.4387	4.1174	1.15486	129.93
200	15.537	864.74	7.854	852.38	2792.5	1940.1	2.33076	6.4312	4.1005	1.15641	127.32
201	15.864	863.57	8.014	856.89	2793.1	1936.2	2.34019	6.4238	4.0836	1.15798	124.77
202	16.197	862.40	8.177	861.40	2793.7	1932.3	2.34961	6.4163	4.0667	1.15955	122.29
203	16.536	861.22	8.343	865.91	2794.2	1928.3	2.35902	6.4089	4.0498	1.16114	119.86
204	16.880	860.04	8.511	870.43	2794.8	1924.4	2.36842	6.4014	4.0330	1.16274	117.49
205	17.229	858.85	8.682	874.96	2795.3	1920.4	2.37781	6.3940	4.0162	1.16435	115.17
206	17.584	857.65	8.856	879.49	2795.8	1916.3	2.38719	6.3866	3.9994	1.16597	112.91
207	17.945	856.45	9.033	884.02	2796.3	1912.3	2.39656	6.3793	3.9827	1.16761	110.70
208	18.311	855.25	9.213	888.56	2796.8	1908.2	2.40591	6.3719	3.9660	1.16925	108.55
209	18.684	854.03	9.395	893.11	2797.3	1904.1	2.41526	6.3646	3.9493	1.17091	106.44
210	19.062	852.82	9.581	897.66	2797.7	1900.0	2.42460	6.3572	3.9326	1.17258	104.38
211	19.446	851.59	9.769	902.22	2798.1	1895.9	2.43393	6.3499	3.9160	1.17427	102.36
212	19.836	850.37	9.961	906.78	2798.6	1891.8	2.44326	6.3426	3.8993	1.17596	100.40
213	20.232	849.13	10.155	911.35	2798.9	1887.6	2.45257	6.3353	3.8827	1.17767	98.47
214	20.634	847.89	10.353	915.93	2799.3	1883.4	2.46187	6.3280	3.8662	1.17939	96.59
215	21.042	846.65	10.554	920.51	2799.7	1879.2	2.47117	6.3208	3.8496	1.18113	94.75
216	21.457	845.40	10.758	925.10	2800.0	1874.9	2.48046	6.3135	3.8331	1.18288	92.96
217	21.878	844.14	10.965	929.69	2800.4	1870.7	2.48974	6.3063	3.8166	1.18464	91.20
218	22.305	842.88	11.176	934.29	2800.7	1866.4	2.49901	6.2991	3.8001	1.18641	89.48
219	22.738	841.61	11.389	938.90	2801.0	1862.1	2.50827	6.2919	3.7836	1.18820	87.80



$t(^{\circ}\text{C})$	$P$ bar	$\rho_l$ kg/m <sup>3</sup>	$\rho_g$ kg/m <sup>3</sup>	$h_f$ kJ/kg	$h_g$ kJ/kg	$\Delta h_g$ kJ/kg	$s_l$ kJ/kg-K	$s_g$ kJ/kg-K	$\Delta S_g$ kJ/kg-K	$v_l$ (m <sup>3</sup> /kg $\times 10^3$ )	$v_g$ (m <sup>3</sup> /kg $\times 10^3$ )
220	23.178	840.34	11.607	943.51	2801.3	1857.8	2.51753	6.2847	3.7671	1.19000	86.16
221	23.625	839.06	11.827	948.13	2801.5	1853.4	2.52678	6.2775	3.7507	1.19182	84.55
222	24.078	837.77	12.052	952.75	2801.8	1849.0	2.53602	6.2703	3.7343	1.19365	82.98
223	24.538	836.48	12.279	957.38	2802.0	1844.6	2.54525	6.2631	3.7179	1.19549	81.44
224	25.005	835.18	12.511	962.02	2802.2	1840.2	2.55448	6.2559	3.7015	1.19735	79.93
225	25.479	833.87	12.745	966.67	2802.4	1835.7	2.56370	6.2488	3.6851	1.19922	78.46
226	25.959	832.56	12.984	971.32	2802.6	1831.2	2.57292	6.2416	3.6687	1.20111	77.02
227	26.446	831.25	13.226	975.98	2802.7	1826.7	2.58212	6.2345	3.6524	1.20301	75.61
228	26.941	829.92	13.472	980.65	2802.9	1822.2	2.59133	6.2274	3.6361	1.20493	74.23
229	27.442	828.59	13.722	985.32	2803.0	1817.7	2.60052	6.2203	3.6197	1.20687	72.88
230	27.951	827.25	13.976	990.00	2803.1	1813.1	2.60971	6.2131	3.6034	1.20882	71.55
231	28.467	825.91	14.233	994.69	2803.1	1808.5	2.61890	6.2060	3.5871	1.21078	70.26
232	28.990	824.56	14.495	999.39	2803.2	1803.8	2.62808	6.1989	3.5709	1.21276	68.99
233	29.521	823.21	14.761	1004.09	2803.2	1799.2	2.63725	6.1918	3.5546	1.21476	67.75
234	30.059	821.84	15.031	1008.80	2803.3	1794.5	2.64642	6.1847	3.5383	1.21678	66.53
235	30.604	820.47	15.304	1013.52	2803.3	1789.7	2.65559	6.1777	3.5221	1.21881	65.34
236	31.157	819.10	15.583	1018.25	2803.2	1785.0	2.66475	6.1706	3.5058	1.22086	64.17
237	31.718	817.71	15.865	1022.98	2803.2	1780.2	2.67390	6.1635	3.4896	1.22292	63.03
238	32.286	816.32	16.152	1027.72	2803.1	1775.4	2.68306	6.1564	3.4734	1.22500	61.91
239	32.863	814.93	16.443	1032.48	2803.1	1770.6	2.69220	6.1494	3.4572	1.22710	60.82
240	33.447	813.52	16.739	1037.24	2803.0	1765.7	2.70135	6.1423	3.4409	1.22922	59.74
241	34.039	812.11	17.039	1042.00	2802.8	1760.8	2.71049	6.1352	3.4247	1.23136	58.69
242	34.639	810.69	17.344	1046.78	2802.7	1755.9	2.71963	6.1282	3.4085	1.23351	57.66
243	35.247	809.27	17.653	1051.57	2802.5	1751.0	2.72876	6.1211	3.3923	1.23569	56.65
244	35.863	807.83	17.967	1056.36	2802.3	1746.0	2.73789	6.1140	3.3761	1.23788	55.66
245	36.488	806.39	18.286	1061.16	2802.1	1741.0	2.74702	6.1070	3.3600	1.24009	54.69
246	37.121	804.94	18.610	1065.98	2801.9	1735.9	2.75615	6.0999	3.3438	1.24232	53.73
247	37.762	803.49	18.939	1070.80	2801.6	1730.8	2.76528	6.0929	3.3276	1.24458	52.80
248	38.412	802.02	19.273	1075.63	2801.4	1725.7	2.77440	6.0858	3.3114	1.24685	51.89
249	39.070	800.55	19.612	1080.47	2801.1	1720.6	2.78352	6.0787	3.2952	1.24914	50.99
250	39.737	799.07	19.956	1085.32	2800.7	1715.4	2.79264	6.0717	3.2790	1.25145	50.111
251	40.412	797.58	20.305	1090.18	2800.4	1710.2	2.80176	6.0646	3.2629	1.25379	49.248
252	41.096	796.09	20.660	1095.05	2800.0	1705.0	2.81088	6.0575	3.2467	1.25614	48.403
253	41.789	794.59	21.020	1099.93	2799.6	1699.7	2.82000	6.0505	3.2305	1.25852	47.573
254	42.491	793.07	21.386	1104.82	2799.2	1694.4	2.82911	6.0434	3.2143	1.26092	46.760
255	43.202	791.55	21.757	1109.72	2798.8	1689.1	2.83823	6.0363	3.1981	1.26334	45.962
256	43.922	790.03	22.134	1114.63	2798.3	1683.7	2.84735	6.0292	3.1819	1.26578	45.180
257	44.651	788.49	22.517	1119.55	2797.8	1678.3	2.85646	6.0222	3.1657	1.26825	44.412
258	45.390	786.94	22.905	1124.48	2797.3	1672.8	2.86558	6.0151	3.1495	1.27074	43.658
259	46.137	785.39	23.300	1129.43	2796.8	1667.4	2.87470	6.0080	3.1333	1.27325	42.919
260	46.895	783.83	23.700	1134.38	2796.2	1661.9	2.88382	6.0009	3.1170	1.27579	42.194
261	47.661	782.25	24.107	1139.34	2795.6	1656.3	2.89294	5.9938	3.1008	1.27836	41.482
262	48.437	780.67	24.520	1144.32	2795.0	1650.7	2.90206	5.9866	3.0846	1.28095	40.783
263	49.223	779.08	24.939	1149.31	2794.4	1645.1	2.91119	5.9795	3.0683	1.28356	40.098
264	50.018	777.48	25.365	1154.31	2793.7	1639.4	2.92031	5.9724	3.0521	1.28620	39.424
265	50.823	775.87	25.797	1159.32	2793.0	1633.7	2.92944	5.9652	3.0358	1.28887	38.764
266	51.638	774.25	26.236	1164.35	2792.3	1628.0	2.93858	5.9581	3.0195	1.29156	38.115
267	52.463	772.63	26.682	1169.38	2791.6	1622.2	2.94771	5.9509	3.0032	1.29429	37.478
268	53.298	770.99	27.135	1174.43	2790.8	1616.3	2.95685	5.9437	2.9869	1.29704	36.853
269	54.143	769.34	27.595	1179.49	2790.0	1610.5	2.96599	5.9365	2.9705	1.29981	36.239
270	54.999	767.68	28.061	1184.57	2789.1	1604.6	2.97514	5.9293	2.9542	1.30262	35.636
271	55.864	766.01	28.536	1189.66	2788.3	1598.6	2.98429	5.9221	2.9378	1.30546	35.044
272	56.740	764.34	29.017	1194.76	2787.4	1592.6	2.99345	5.9149	2.9215	1.30833	34.462
273	57.627	762.65	29.506	1199.87	2786.5	1586.6	3.00261	5.9077	2.9051	1.31122	33.891
274	58.524	760.95	30.003	1205.00	2785.5	1580.5	3.01178	5.9004	2.8886	1.31415	33.330

$t(^{\circ}\text{C})$	$P$ bar	$\rho_l$ kg/m <sup>3</sup>	$\rho_g$ kg/m <sup>3</sup>	$h_f$ kJ/kg	$h_g$ kJ/kg	$\Delta h_{fg}$ kJ/kg	$s_f$ kJ/kg-K	$s_g$ kJ/kg-K	$\Delta S_{fg}$ kJ/kg-K	$v_f$ (m <sup>3</sup> /kg $\times 10^3$ )	$v_g$ (m <sup>3</sup> /kg $\times 10^3$ )
275	59.431	759.24	30.507	1210.15	2784.5	1574.4	3.02095	5.8931	2.8722	1.31711	32.779
276	60.350	757.52	31.020	1215.30	2783.5	1568.2	3.03013	5.8859	2.8557	1.32011	32.237
277	61.279	755.78	31.541	1220.47	2782.5	1562.0	3.03931	5.8786	2.8392	1.32313	31.705
278	62.219	754.04	32.069	1225.66	2781.4	1555.8	3.04850	5.8712	2.8227	1.32619	31.182
279	63.170	752.28	32.607	1230.86	2780.3	1549.4	3.05770	5.8639	2.8062	1.32929	30.669
280	64.132	750.52	33.152	1236.08	2779.2	1543.1	3.06691	5.8565	2.7896	1.33242	30.164
281	65.105	748.74	33.707	1241.31	2778.0	1536.7	3.07613	5.8492	2.7730	1.33558	29.668
282	66.089	746.95	34.270	1246.56	2776.8	1530.2	3.08535	5.8418	2.7564	1.33878	29.180
283	67.085	745.14	34.843	1251.82	2775.5	1523.7	3.09458	5.8344	2.7398	1.34202	28.701
284	68.092	743.33	35.424	1257.10	2774.3	1517.2	3.10382	5.8269	2.7231	1.34530	28.229
285	69.111	741.50	36.015	1262.40	2773.0	1510.6	3.11308	5.8195	2.7064	1.34862	27.766
286	70.141	739.66	36.616	1267.71	2771.6	1503.9	3.12234	5.8120	2.6896	1.35197	27.310
287	71.183	737.81	37.226	1273.04	2770.2	1497.2	3.13161	5.8045	2.6729	1.35537	26.863
288	72.237	735.94	37.847	1278.39	2768.8	1490.4	3.14089	5.7969	2.6560	1.35881	26.422
289	73.303	734.06	38.478	1283.75	2767.4	1483.6	3.15019	5.7894	2.6392	1.36229	25.989
290	74.380	732.16	39.119	1289.14	2765.9	1476.7	3.15950	5.7818	2.6223	1.36581	25.563
291	75.470	730.26	39.770	1294.54	2764.3	1469.8	3.16882	5.7742	2.6054	1.36938	25.144
292	76.572	728.33	40.433	1299.96	2762.8	1462.8	3.17815	5.7665	2.5884	1.37300	24.732
293	77.686	726.40	41.106	1305.40	2761.2	1455.8	3.18750	5.7589	2.5714	1.37666	24.327
294	78.813	724.45	41.791	1310.86	2759.5	1448.7	3.19686	5.7511	2.5543	1.38037	23.928
295	79.952	722.48	42.488	1316.34	2757.8	1441.5	3.20623	5.7434	2.5372	1.38412	23.536
296	81.103	720.50	43.196	1321.84	2756.1	1434.3	3.21563	5.7356	2.5200	1.38793	23.150
297	82.268	718.50	43.917	1327.36	2754.3	1427.0	3.22503	5.7278	2.5028	1.39179	22.770
298	83.445	716.49	44.650	1332.90	2752.5	1419.6	3.23446	5.7200	2.4855	1.39570	22.397
299	84.635	714.46	45.395	1338.47	2750.7	1412.2	3.24390	5.7121	2.4682	1.39967	22.029
300	85.838	712.41	46.154	1344.05	2748.7	1404.7	3.25336	5.7042	2.4508	1.40369	21.667
301	87.054	710.35	46.926	1349.66	2746.8	1397.1	3.26284	5.6962	2.4334	1.40777	21.310
302	88.283	708.27	47.711	1355.29	2744.8	1389.5	3.27233	5.6882	2.4159	1.41190	20.960
303	89.526	706.17	48.510	1360.95	2742.8	1381.8	3.28185	5.6802	2.3983	1.41610	20.614
304	90.782	704.05	49.324	1366.63	2740.7	1374.0	3.29139	5.6721	2.3807	1.42035	20.274
305	92.051	701.92	50.15	1372.33	2738.5	1366.2	3.30095	5.6640	2.3630	1.42467	19.940
306	93.334	699.76	51.00	1378.06	2736.3	1358.3	3.31053	5.6558	2.3453	1.42906	19.610
307	94.631	697.59	51.85	1383.81	2734.1	1350.3	3.32014	5.6476	2.3275	1.43351	19.285
308	95.942	695.40	52.73	1389.59	2731.8	1342.2	3.32977	5.6393	2.3096	1.43803	18.966
309	97.267	693.18	53.62	1395.40	2729.4	1334.0	3.33943	5.6310	2.2916	1.44262	18.651
310	98.605	690.95	54.52	1401.23	2727.0	1325.8	3.34911	5.6226	2.2735	1.44728	18.340
311	99.958	688.70	55.45	1407.10	2724.6	1317.5	3.35882	5.6142	2.2554	1.45202	18.035
312	101.326	686.42	56.39	1412.99	2722.1	1309.1	3.36856	5.6057	2.2372	1.45683	17.734
313	102.707	684.12	57.35	1418.91	2719.5	1300.6	3.37832	5.5972	2.2189	1.46173	17.437
314	104.104	681.80	58.33	1424.86	2716.9	1292.0	3.38812	5.5886	2.2005	1.46670	17.145
315	105.51	679.46	59.32	1430.84	2714.2	1283.3	3.39795	5.5799	2.1820	1.47176	16.856
316	106.94	677.09	60.34	1436.86	2711.4	1274.6	3.40781	5.5712	2.1634	1.47691	16.572
317	108.38	674.70	61.38	1442.90	2708.6	1265.7	3.41770	5.5624	2.1447	1.48215	16.293
318	109.84	672.28	62.44	1448.99	2705.7	1256.7	3.42763	5.5535	2.1259	1.48748	16.017
319	111.31	669.83	63.51	1455.10	2702.8	1247.6	3.43760	5.5446	2.1070	1.49291	15.745
320	112.79	667.36	64.62	1461.25	2699.7	1238.5	3.44760	5.5356	2.0880	1.49843	15.476
321	114.29	664.87	65.74	1467.44	2696.6	1229.2	3.45765	5.5265	2.0688	1.50406	15.212
322	115.81	662.34	66.89	1473.67	2693.5	1219.8	3.46773	5.5173	2.0496	1.50980	14.951
323	117.34	659.78	68.06	1479.93	2690.2	1210.3	3.47786	5.5081	2.0302	1.51565	14.693
324	118.89	657.20	69.26	1486.24	2686.9	1200.7	3.48803	5.4987	2.0107	1.52161	14.439
325	120.46	654.58	70.48	1492.58	2683.5	1190.9	3.49825	5.4893	1.9911	1.52769	14.189
326	122.04	651.93	71.73	1498.97	2680.1	1181.1	3.50852	5.4798	1.9713	1.53390	13.942
327	123.64	649.25	73.00	1505.40	2676.5	1171.1	3.51884	5.4702	1.9513	1.54024	13.698
328	125.25	646.53	74.31	1511.88	2672.9	1161.0	3.52921	5.4605	1.9313	1.54671	13.457
329	126.88	643.78	75.65	1518.41	2669.1	1150.7	3.53963	5.4506	1.9110	1.55332	13.219

$t(^{\circ}\text{C})$	$P$ bar	$\rho_l$ kg/m <sup>3</sup>	$\rho_g$ kg/m <sup>3</sup>	$h_f$ kJ/kg	$h_g$ kJ/kg	$\Delta h_{fg}$ kJ/kg	$s_f$ kJ/kg-K	$s_g$ kJ/kg-K	$\Delta s_{fg}$ kJ/kg-K	$v_f$ (m <sup>3</sup> /kg $\times 10^3$ )	$v_g$ (m <sup>3</sup> /kg $\times 10^3$ )
330	128.52	641.0	77.01	1525.0	2665.3	1140.3	3.5501	5.4407	1.8906	1.5601	12.985
331	130.19	638.2	78.41	1531.6	2661.4	1129.8	3.5607	5.4307	1.8700	1.5670	12.753
332	131.87	635.3	79.84	1538.3	2657.4	1119.1	3.5713	5.4205	1.8493	1.5740	12.524
333	133.57	632.4	81.31	1545.0	2653.3	1108.3	3.5819	5.4103	1.8283	1.5813	12.298
334	135.28	629.5	82.82	1551.8	2649.0	1097.2	3.5927	5.3999	1.8072	1.5887	12.075
335	137.01	626.5	84.36	1558.6	2644.7	1086.1	3.6035	5.3894	1.7859	1.5963	11.854
336	138.76	623.4	85.94	1565.5	2640.3	1074.7	3.6144	5.3787	1.7643	1.6040	11.636
337	140.53	620.3	87.56	1572.5	2635.7	1063.2	3.6253	5.3679	1.7426	1.6120	11.421
338	142.32	617.2	89.22	1579.5	2631.1	1051.5	3.6364	5.3569	1.7205	1.6202	11.208
339	144.12	614.0	90.93	1586.7	2626.3	1039.6	3.6475	5.3458	1.6983	1.6286	10.997
340	145.94	610.8	92.69	1593.8	2621.3	1027.5	3.6587	5.3345	1.6758	1.6373	10.788
341	147.78	607.5	94.50	1601.1	2616.3	1015.2	3.6701	5.3231	1.6530	1.6462	10.582
342	149.64	604.1	96.36	1608.4	2611.1	1002.7	3.6815	5.3114	1.6299	1.6553	10.378
343	151.52	600.7	98.27	1615.8	2605.7	989.9	3.6930	5.2996	1.6066	1.6647	10.176
344	153.42	597.2	100.24	1623.3	2600.2	976.9	3.7047	5.2876	1.5829	1.6745	9.976
345	155.33	593.7	102.27	1630.9	2594.5	963.6	3.7164	5.2753	1.5589	1.6845	9.778
346	157.27	590.0	104.37	1638.6	2588.7	950.1	3.7283	5.2629	1.5345	1.6948	9.581
347	159.22	586.3	106.53	1646.4	2582.7	936.3	3.7404	5.2502	1.5098	1.7056	9.387
348	161.20	582.5	108.77	1654.3	2576.5	922.2	3.7526	5.2372	1.4847	1.7166	9.194
349	163.20	578.7	111.08	1662.3	2570.1	907.8	3.7649	5.2240	1.4591	1.7281	9.002
350	165.21	574.7	113.48	1670.4	2563.5	893.0	3.7774	5.2105	1.4331	1.7401	8.812
351	167.25	570.6	115.96	1678.7	2556.6	877.9	3.7901	5.1967	1.4066	1.7525	8.623
352	169.31	566.4	118.54	1687.1	2549.6	862.4	3.8030	5.1825	1.3796	1.7654	8.436
353	171.38	562.2	121.22	1695.7	2542.2	846.6	3.8161	5.1681	1.3520	1.7788	8.249
354	173.48	557.8	124.01	1704.4	2534.6	830.2	3.8294	5.1532	1.3238	1.7929	8.064
355	175.61	553.2	126.92	1713.3	2526.7	813.5	3.8429	5.1379	1.2950	1.8076	7.879
356	177.75	548.5	129.95	1722.4	2518.5	796.2	3.8568	5.1222	1.2655	1.8230	7.695
357	179.92	543.7	133.13	1731.7	2510.0	778.3	3.8709	5.1060	1.2352	1.8392	7.512
358	182.11	538.7	136.46	1741.2	2501.1	759.9	3.8853	5.0893	1.2040	1.8563	7.328
359	184.32	533.5	139.96	1750.9	2491.8	740.8	3.9001	5.0721	1.1719	1.8744	7.145
360	186.55	528.1	143.65	1761.0	2482.0	721.1	3.9153	5.0542	1.1388	1.8936	6.962
361	188.81	522.5	147.54	1771.3	2471.8	700.5	3.9310	5.0355	1.1046	1.9140	6.778
362	191.10	516.6	151.68	1782.0	2461.0	679.0	3.9471	5.0161	1.0690	1.9358	6.593
363	193.40	510.4	156.08	1793.1	2449.6	656.5	3.9638	4.9958	1.0320	1.9592	6.407
364	195.74	503.9	160.80	1804.6	2437.5	632.9	3.9812	4.9745	0.9933	1.9845	6.219
365.0	198.09	497.0	165.88	1816.7	2424.6	607.9	3.9994	4.9520	0.9526	2.0120	6.028
365.5	199.28	493.4	168.58	1822.9	2417.8	594.8	4.0088	4.9402	0.9314	2.0268	5.932
366.0	200.48	489.7	171.39	1829.3	2410.7	581.3	4.0185	4.9280	0.9096	2.0422	5.835
366.5	201.68	485.8	174.33	1835.9	2403.3	567.4	4.0284	4.9155	0.8870	2.0585	5.736
367.0	202.89	481.8	177.42	1842.7	2395.6	552.9	4.0387	4.9024	0.8637	2.0757	5.636
367.5	204.11	477.6	180.67	1849.8	2387.6	537.8	4.0493	4.8888	0.8395	2.0939	5.535
368.0	205.33	473.2	184.11	1857.1	2379.2	522.1	4.0602	4.8746	0.8143	2.1133	5.432
368.5	206.56	468.6	187.75	1864.7	2370.3	505.6	4.0717	4.8597	0.7880	2.1340	5.326
369.0	207.80	463.8	191.63	1872.6	2360.9	488.3	4.0836	4.8440	0.7604	2.1563	5.218
369.5	209.05	458.6	195.79	1880.9	2350.9	470.0	4.0962	4.8274	0.7313	2.1804	5.107
370.0	210.30	453.1	200.29	1889.7	2340.2	450.4	4.1094	4.8098	0.7003	2.2068	4.993
370.5	211.56	447.2	205.21	1899.1	2328.5	429.4	4.1236	4.7907	0.6671	2.2361	4.873
371.0	212.83	440.7	210.64	1909.3	2315.8	406.5	4.1389	4.7700	0.6311	2.2689	4.747
371.5	214.11	433.5	216.74	1920.5	2301.6	381.2	4.1558	4.7471	0.5913	2.3067	4.614
372.0	215.39	425.3	223.74	1933.0	2285.5	352.5	4.1748	4.7212	0.5464	2.3515	4.469
372.5	216.69	415.4	232.1	1947.7	2266.6	318.9	4.1971	4.6910	0.4939	2.4074	4.309
373.0	217.99	402.4	242.7	1966.6	2243.0	276.4	4.2258	4.6536	0.4277	2.4850	4.121
373.5	219.30	385.0	259.0	1991.6	2207.3	215.7	4.2640	4.5977	0.3337	2.5974	3.861
373.976	220.55	322		2086		0	4.409		0	3.106	

Source: Reprinted from NBS/NRC Steam Tables by L. Haar, et al., New York: Hemisphere, 1984, pp. 9-16; with permission.

## APPENDIX B: Density Tables for NaCl in H<sub>2</sub>O as a Function of Temperature, Pressure and Salinity –From Ref. 7 –

TEMP (°C)	PRESS (BAR)	MOLALITY								
		.1000	.2500	.5000	.7500	1.0000	2.0000	3.0000	4.0000	5.0000
0	1	.995732	.989259	.978889	.968991	.959525	.925426	.896292	.870996	.848646
10	1	.995998	.989781	.979804	.970256	.961101	.927905	.899262	.874201	.851958
20	1	.997620	.991564	.981833	.972505	.963594	.930909	.902565	.877643	.855469
25	1	.998834	.992832	.983185	.973932	.965038	.932590	.904339	.879457	.857301
30	1	1.000279	.994319	.984735	.975539	.966649	.934382	.906194	.881334	.859195
40	1	1.003796	.997883	.988374	.979243	.970455	.938287	.910145	.885276	.863108
50	1	1.008064	1.002161	.992668	.983551	.974772	.942603	.914411	.889473	.867241
50	1	1.0081	1.0022	.9927	.9836	.9748	.9427	.9145	.8895	.8673
60	1	1.0130	1.0071	.9976	.9885	.9797	.9474	.9191	.8940	.8716
70	1	1.0186	1.0127	1.0031	.9939	.9851	.9526	.9240	.8987	.8762
80	1	1.0249	1.0188	1.0092	.9999	.9909	.9581	.9293	.9037	.8809
90	1	1.0317	1.0256	1.0157	1.0063	.9972	.9640	.9348	.9089	.8858
100	1	1.0391	1.0329	1.0228	1.0133	1.0040	.9703	.9406	.9144	.8910
110	1	1.0471	1.0407	1.0305	1.0207	1.0113	.9769	.9468	.9201	.8964
120	2	1.0557	1.0491	1.0386	1.0286	1.0190	.9839	.9532	.9261	.9020
130	3	1.0649	1.0582	1.0474	1.0371	1.0272	.9912	.9599	.9323	.9078
140	4	1.0748	1.0678	1.0567	1.0461	1.0359	.9990	.9670	.9388	.9139
150	5	1.0854	1.0781	1.0666	1.0556	1.0452	1.0072	.9744	.9456	.9202
160	6	1.0966	1.0891	1.0771	1.0658	1.0550	1.0159	.9821	.9527	.9267
170	8	1.1087	1.1008	1.0884	1.0766	1.0654	1.0250	.9903	.9601	.9335
180	10	1.1215	1.1133	1.1003	1.0881	1.0765	1.0347	.9989	.9678	.9406
190	13	1.1353	1.1266	1.1131	1.1004	1.0883	1.0449	1.0079	.9759	.9479
200	16	1.1500	1.1409	1.1268	1.1134	1.1008	1.0558	1.0175	.9844	.9556
210	19	1.1658	1.1562	1.1413	1.1274	1.1142	1.0673	1.0276	.9933	.9635
220	23	1.1828	1.1727	1.1570	1.1424	1.1286	1.0796	1.0382	1.0027	.9718
230	28	1.2011	1.1904	1.1738	1.1584	1.1440	1.0927	1.0496	1.0125	.9804
240	33	1.2209	1.2095	1.1920	1.1757	1.1605	1.1068	1.0616	1.0229	.9893
250	40	1.2425	1.2303	1.2116	1.1944	1.1783	1.1218	1.0744	1.0338	.9986
260	47	1.2661	1.2529	1.2330	1.2146	1.1976	1.1379	1.0881	1.0454	1.0082
270	55	1.2920	1.2777	1.2562	1.2366	1.2184	1.1552	1.1027	1.0575	1.0182
280	64	1.3206	1.3050	1.2817	1.2604	1.2411	1.1749	1.1182	1.0704	1.0286
290	74	1.3526	1.3353	1.3097	1.2868	1.2657	1.1938	1.1347	1.0839	1.0394
300	86	1.3886	1.3691	1.3407	1.3155	1.2926	1.2151	1.1520	1.0979	1.0504

TEMP (°C)	PRESS (BAR)	MOLALITY								
		.1000	.2500	.5000	.7500	1.0000	2.0000	3.0000	4.0000	5.0000
0	200	.986107	.979894	.969737	.960426	.951324	.918469			
10	200	.986943	.980946	.971317	.962097	.953251	.921123			
20	200	.988895	.983034	.973513	.964577	.955893	.924219			
25	200	.990212	.984397	.975097	.966075	.957446	.925922	.898408	.874105	.852393
30	200	.991729	.985950	.976553	.967728	.959139	.927724	.900255	.875964	.854257
40	200	.995310	.989570	.980336	.971464	.962921	.931614	.904167	.879856	.858128
50	200	.999554	.993820	.984597	.975734	.967196	.935872	.908366	.883982	.862192
50	200	.9996	.9938	.9846	.9758	.9672	.9359	.9084	.8840	.8622
60	200	1.0044	.9987	.9894	.9805	.9720	.9405	.9129	.8884	.8664
70	200	1.0098	1.0041	.9947	.9858	.9772	.9455	.9177	.8929	.8708
80	200	1.0158	1.0100	1.0005	.9915	.9828	.9508	.9227	.8977	.8754
90	200	1.0224	1.0164	1.0069	.9977	.9888	.9565	.9280	.9027	.8802
100	200	1.0294	1.0233	1.0136	1.0043	.9953	.9624	.9335	.9080	.8852
110	200	1.0370	1.0308	1.0209	1.0113	1.0022	.9687	.9394	.9134	.8903
120	200	1.0452	1.0388	1.0286	1.0188	1.0095	.9753	.9455	.9191	.8957
130	200	1.0539	1.0473	1.0368	1.0268	1.0172	.9823	.9518	.9250	.9013
140	200	1.0631	1.0563	1.0455	1.0353	1.0254	.9896	.9585	.9312	.9071
150	200	1.0730	1.0660	1.0548	1.0442	1.0341	.9973	.9655	.9376	.9131
160	200	1.0835	1.0762	1.0647	1.0537	1.0432	1.0054	.9728	.9443	.9194
170	200	1.0947	1.0871	1.0751	1.0637	1.0529	1.0139	.9804	.9513	.9259
180	200	1.1066	1.0987	1.0862	1.0744	1.0632	1.0229	.9885	.9586	.9326
190	200	1.1192	1.1110	1.0980	1.0857	1.0741	1.0324	.9969	.9663	.9397
200	200	1.1327	1.1241	1.1105	1.0978	1.0857	1.0425	1.0058	.9743	.9470
210	200	1.1472	1.1381	1.1239	1.1106	1.0980	1.0531	1.0152	.9827	.9547
220	200	1.1627	1.1531	1.1383	1.1243	1.1112	1.0645	1.0251	.9915	.9624
230	200	1.1794	1.1693	1.1536	1.1390	1.1253	1.0766	1.0357	1.0008	.9709
240	200	1.1973	1.1867	1.1702	1.1548	1.1404	1.0896	1.0470	1.0107	.9796
250	200	1.2168	1.2055	1.1880	1.1719	1.1567	1.1035	1.0590	1.0211	.9887
260	200	1.2380	1.2259	1.2074	1.1904	1.1744	1.1185	1.0719	1.0322	.9981
270	200	1.2613	1.2483	1.2286	1.2105	1.1936	1.1348	1.0858	1.0441	1.0081
280	200	1.2869	1.2729	1.2517	1.2325	1.2146	1.1524	1.1008	1.0567	1.0185
290	200	1.3154	1.3001	1.2773	1.2566	1.2375	1.1716	1.1170	1.0702	1.0295
300	200	1.3476	1.3307	1.3057	1.2833	1.2628	1.1925	1.1345	1.0846	1.0410

TEMP (°C)	PRESS (BAR)	MOLALITY								
		.1000	.2500	.5000	.7500	1.0000	2.0000	3.0000	4.0000	5.0000
0	400	.977044	.971070	.961490	.952335	.943568	.911854			
10	400	.978376	.972581	.963271	.954353	.945792	.914647			
20	400	.980625	.974942	.965896	.957038	.948608	.917820			
25	400	.982037	.976394	.967316	.958601	.950215	.919544	.892715	.868956	.847668
30	400	.983622	.978008	.968974	.960297	.951944	.921355	.894554	.870797	.849512
40	400	.987267	.981686	.972702	.964068	.955750	.925234	.898430	.874641	.853332
50	400	.991498	.985919	.976942	.968310	.959992	.929443	.902569	.878700	.857327
50	400	.9915	.9859	.9770	.9683	.9600	.9295	.9026	.8787	.8574
60	400	.9963	.9907	.9817	.9730	.9647	.9340	.9070	.8829	.8615
70	400	1.0016	.9959	.9869	.9781	.9697	.9388	.9116	.8874	.8658
80	400	1.0074	1.0016	.9925	.9837	.9752	.9439	.9165	.8920	.8702
90	400	1.0136	1.0078	.9985	.9896	.9810	.9494	.9216	.8969	.8748
100	400	1.0204	1.0145	1.0050	.9959	.9872	.9551	.9269	.9019	.8796
110	400	1.0276	1.0216	1.0119	1.0026	.9937	.9611	.9325	.9071	.8846
120	400	1.0353	1.0291	1.0192	1.0098	1.0006	.9674	.9383	.9126	.8897
130	400	1.0436	1.0372	1.0270	1.0173	1.0080	.9740	.9443	.9182	.8951
140	400	1.0523	1.0457	1.0352	1.0252	1.0157	.9809	.9506	.9241	.9006
150	400	1.0615	1.0547	1.0439	1.0336	1.0238	.9881	.9572	.9302	.9064
160	400	1.0713	1.0643	1.0531	1.0425	1.0323	.9957	.9641	.9365	.9123
170	400	1.0816	1.0743	1.0628	1.0518	1.0413	1.0036	.9712	.9431	.9185
180	400	1.0926	1.0850	1.0730	1.0617	1.0508	1.0119	.9787	.9499	.9249
190	400	1.1042	1.0963	1.0838	1.0720	1.0608	1.0207	.9865	.9571	.9315
200	400	1.1165	1.1082	1.0953	1.0830	1.0714	1.0299	.9947	.9645	.9384
210	400	1.1296	1.1209	1.1074	1.0946	1.0826	1.0396	1.0033	.9723	.9456
220	400	1.1434	1.1344	1.1202	1.1070	1.0944	1.0498	1.0123	.9804	.9531
230	400	1.1582	1.1487	1.1339	1.1201	1.1070	1.0607	1.0218	.9889	.9608
240	400	1.1740	1.1640	1.1485	1.1340	1.1203	1.0722	1.0319	.9979	.9689
250	400	1.1908	1.1803	1.1640	1.1489	1.1346	1.0845	1.0426	1.0073	.9773
260	400	1.2089	1.1978	1.1807	1.1648	1.1499	1.0976	1.0541	1.0173	.9861
270	400	1.2284	1.2166	1.1986	1.1819	1.1663	1.1117	1.0663	1.0279	.9953
280	400	1.2494	1.2369	1.2179	1.2004	1.1840	1.1269	1.0794	1.0392	1.0050
290	400	1.2723	1.2590	1.2388	1.2204	1.2032	1.1433	1.0935	1.0512	1.0151
300	400	1.2972	1.2830	1.2616	1.2421	1.2240	1.1612	1.1089	1.0642	1.0257

TEMP (°C)	PRESS (BAR)	MOLALITY									
		.1000	.2500	.5000	.7500	1.0000	2.0000	3.0000	4.0000	5.0000	
0	600	.968527	.962771	.953537	.944706	.936244	.905577				
10	600	.970289	.964678	.955661	.947019	.938718	.908479				
20	600	.972800	.967282	.958405	.949884	.941687	.911717				
25	600	.974299	.968812	.959983	.951504	.943341	.913457	.887267	.864024	.843145	
30	600	.975946	.970483	.961690	.953240	.945103	.915277	.889098	.865848	.844970	
40	600	.979655	.974217	.965462	.957045	.948933	.919146	.892942	.869647	.848740	
50	600	.983879	.978442	.969688	.961268	.953151	.923312	.897026	.873642	.852668	
50	600	.9839	.9784	.9697	.9613	.9532	.9233	.8970	.8736	.8527	
60	600	.9886	.9831	.9743	.9659	.9577	.9278	.9013	.8778	.8567	
70	600	.9938	.9883	.9794	.9709	.9627	.9325	.9058	.8821	.8609	
80	600	.9994	.9938	.9849	.9763	.9680	.9375	.9106	.8867	.8653	
90	600	1.0055	.9998	.9907	.9820	.9736	.9427	.9155	.8913	.8697	
100	600	1.0119	1.0062	.9970	.9881	.9795	.9482	.9207	.8962	.8744	
110	600	1.0189	1.0130	1.0036	.9945	.9858	.9540	.9260	.9013	.8792	
120	600	1.0262	1.0202	1.0106	1.0013	.9925	.9600	.9316	.9065	.8841	
130	600	1.0340	1.0279	1.0180	1.0085	.9994	.9663	.9374	.9119	.8893	
140	600	1.0423	1.0359	1.0258	1.0161	1.0068	.9729	.9434	.9175	.8946	
150	600	1.0510	1.0444	1.0340	1.0240	1.0145	.9798	.9497	.9233	.9001	
160	600	1.0602	1.0534	1.0426	1.0323	1.0225	.9869	.9562	.9294	.9058	
170	600	1.0699	1.0628	1.0517	1.0411	1.0310	.9944	.9630	.9356	.9117	
180	600	1.0801	1.0728	1.0612	1.0503	1.0398	1.0022	.9700	.9421	.9177	
190	600	1.0908	1.0832	1.0713	1.0599	1.0492	1.0104	.9773	.9488	.9241	
200	600	1.1021	1.0943	1.0818	1.0701	1.0589	1.0189	.9850	.9558	.9306	
210	600	1.1141	1.1059	1.0930	1.0808	1.0692	1.0279	.9929	.9630	.9374	
220	600	1.1267	1.1182	1.1047	1.0920	1.0800	1.0373	1.0013	.9706	.9444	
230	600	1.1401	1.1311	1.1171	1.1039	1.0914	1.0472	1.0100	.9785	.9517	
240	600	1.1542	1.1448	1.1302	1.1165	1.1035	1.0576	1.0192	.9867	.9592	
250	600	1.1692	1.1594	1.1441	1.1298	1.1163	1.0686	1.0289	.9954	.9671	
260	600	1.1852	1.1748	1.1588	1.1439	1.1298	1.0803	1.0391	1.0044	.9753	
270	600	1.2021	1.1913	1.1745	1.1589	1.1443	1.0928	1.0500	1.0140	.9838	
280	600	1.2203	1.2088	1.1913	1.1750	1.1597	1.1061	1.0616	1.0241	.9927	
290	600	1.2397	1.2276	1.2092	1.1922	1.1763	1.1204	1.0740	1.0349	1.0020	
300	600	1.2605	1.2478	1.2285	1.2107	1.1941	1.1359	1.0875	1.0465	1.0118	

TEMP (°C)	PRESS (BAR)	MOLALITY								
		.1000	.2500	.5000	.7500	1.0000	2.0000	3.0000	4.0000	5.0000
0	800	.960519	.954961	.946041	.937506	.929323	.899616			
10	800	.962645	.957201	.948451	.940061	.932000	.902598			
20	800	.965383	.960014	.951375	.943079	.935097	.905884			
25	800	.966958	.961614	.953013	.944750	.936793	.907639	.882050	.859300	.8388
30	800	.968661	.963336	.954762	.946522	.938584	.909464	.883872	.861107	.8406
40	800	.972428	.967122	.958577	.950358	.942436	.913324	.887686	.864862	.8443
50	800	.976651	.971342	.962792	.954567	.946634	.917453	.891718	.868797	.8482
50	800	.9767	.9713	.9628	.9546	.9466	.9175	.8917	.8688	.8482
60	800	.9813	.9760	.9674	.9591	.9512	.9218	.8959	.8729	.8522
70	800	.9864	.9810	.9724	.9640	.9560	.9265	.9004	.8771	.8563
80	800	.9919	.9864	.9777	.9693	.9612	.9313	.9050	.8816	.8606
90	800	.9977	.9922	.9834	.9749	.9666	.9365	.9098	.8861	.8649
100	800	1.0040	.9984	.9894	.9808	.9724	.9418	.9149	.8909	.8695
110	800	1.0107	1.0050	.9958	.9870	.9785	.9474	.9201	.8958	.8741
120	800	1.0177	1.0119	1.0025	.9935	.9849	.9532	.9255	.9009	.8789
130	800	1.0252	1.0192	1.0096	1.0004	.9916	.9593	.9311	.9061	.8839
140	800	1.0330	1.0269	1.0170	1.0076	.9986	.9657	.9369	.9115	.8890
150	800	1.0413	1.0350	1.0249	1.0152	1.0060	.9723	.9429	.9171	.8943
160	800	1.0500	1.0435	1.0330	1.0231	1.0136	.9791	.9492	.9229	.8997
170	800	1.0591	1.0524	1.0416	1.0314	1.0216	.9862	.9556	.9289	.9054
180	800	1.0687	1.0617	1.0506	1.0401	1.0300	.9937	.9623	.9351	.9112
190	800	1.0787	1.0715	1.0600	1.0492	1.0388	1.0014	.9693	.9415	.9172
200	800	1.0893	1.0818	1.0699	1.0587	1.0479	1.0094	.9765	.9481	.9234
210	800	1.1004	1.0926	1.0802	1.0686	1.0575	1.0178	.9840	.9550	.9298
220	800	1.1120	1.1039	1.0911	1.0790	1.0676	1.0266	.9919	.9621	.9365
230	800	1.1243	1.1158	1.1025	1.0900	1.0781	1.0358	1.0000	.9645	.9384
240	800	1.1371	1.1283	1.1145	1.1015	1.0892	1.0454	1.0085	.9772	.9505
250	800	1.1507	1.1415	1.1271	1.1136	1.1008	1.0555	1.0174	.9852	.9579
260	800	1.1651	1.1554	1.1404	1.1264	1.1131	1.0661	1.0267	.9935	.9655
270	800	1.1802	1.1701	1.1545	1.1399	1.1261	1.0773	1.0366	1.0023	.9735
280	800	1.1962	1.1857	1.1694	1.1541	1.1398	1.0892	1.0470	1.0115	.9817
290	800	1.2132	1.2022	1.1852	1.1693	1.1544	1.1019	1.0580	1.0212	.9904
300	800	1.2313	1.2197	1.2020	1.1855	1.1700	1.1155	1.0699	1.0315	.9994



TEMP (°C)	PRESS (BAR)	MOLALITY								
		.1000	.2500	.5000	.7500	1.0000	2.0000	3.0000	4.0000	5.0000
0	1000	.952997	.947618	.938982	.930716	.922786	.893956			
10	1000	.955416	.950125	.941619	.933460	.925617	.896986			
20	1000	.958344	.953112	.944690	.936602	.928817	.900307			
25	1000	.959984	.954771	.946379	.938314	.930547	.902071	.877050	.854776	.834697
30	1000	.961734	.956536	.948165	.940116	.932362	.903900	.878863	.856567	.836484
40	1000	.965552	.960367	.952015	.943979	.936232	.907750	.882646	.860279	.840156
50	1000	.969775	.964584	.956222	.948174	.940412	.911844	.886630	.864156	.843954
50	1000	.9698	.9646	.9562	.9482	.9404	.9119	.8866	.8641	.8439
60	1000	.9744	.9692	.9608	.9527	.9449	.9162	.8908	.8682	.8479
70	1000	.9794	.9741	.9657	.9575	.9497	.9208	.8952	.8724	.8520
80	1000	.9847	.9794	.9709	.9627	.9547	.9255	.8997	.8768	.8561
90	1000	.9905	.9851	.9764	.9681	.9601	.9306	.9045	.8813	.8604
100	1000	.9965	.9911	.9823	.9739	.9657	.9358	.9094	.8859	.8648
110	1000	1.0030	.9974	.9885	.9799	.9716	.9413	.9145	.8907	.8694
120	1000	1.0098	1.0041	.9950	.9862	.9778	.9470	.9198	.8957	.8741
130	1000	1.0169	1.0111	1.0018	.9929	.9843	.9529	.9253	.9008	.8789
140	1000	1.0244	1.0185	1.0090	.9999	.9911	.9591	.9310	.9061	.8838
150	1000	1.0323	1.0262	1.0164	1.0071	.9982	.9655	.9368	.9115	.8889
160	1000	1.0406	1.0343	1.0243	1.0147	1.0055	.9721	.9429	.9171	.8942
170	1000	1.0492	1.0427	1.0324	1.0226	1.0132	.9790	.9492	.9229	.8996
180	1000	1.0582	1.0516	1.0410	1.0309	1.0212	.9861	.9556	.9289	.9052
190	1000	1.0677	1.0608	1.0499	1.0395	1.0296	.9935	.9623	.9350	.9110
200	1000	1.0776	1.0705	1.0592	1.0485	1.0383	1.0012	.9693	.9414	.9169
210	1000	1.0880	1.0806	1.0689	1.0579	1.0473	1.0092	.9765	.9480	.9230
220	1000	1.0988	1.0912	1.0791	1.0677	1.0568	1.0176	.9839	.9548	.9294
230	1000	1.1102	1.1022	1.0897	1.0779	1.0667	1.0262	.9916	.9618	.9359
240	1000	1.1221	1.1138	1.1008	1.0886	1.0770	1.0353	.9997	.9691	.9427
250	1000	1.1345	1.1260	1.1125	1.0998	1.0878	1.0447	1.0080	.9766	.9496
260	1000	1.1474	1.1387	1.1247	1.1116	1.0991	1.0545	1.0167	.9844	.9568
270	1000	1.1614	1.1521	1.1375	1.1239	1.1110	1.0649	1.0258	.9926	.9643
280	1000	1.1758	1.1661	1.1510	1.1369	1.1235	1.0757	1.0354	1.0011	.9720
290	1000	1.1911	1.1810	1.1652	1.1505	1.1366	1.0871	1.0454	1.0099	.9801
300	1000	1.2071	1.1966	1.1802	1.1650	1.1506	1.0993	1.0560	1.0192	.9884

## APPENDIX C: Density Probe Specifications

The Cole-Palmer Low-Cost Specific Gravity Meter, 1.000 to 1.300 SGU, ° C model works on the basis of pressure differentials. Because hydrostatic pressure is dependent on the density, as seen in Equation C-1

$$P(z) = \rho g z + P_0 \quad (C-1)$$

where  $\rho$  is the density,  $g$  is the acceleration due to gravity,  $z$  is a depth at which a pressure  $P$  is measured with respect to a reference pressure,  $P_0$ . By measuring the pressure at two locations and thus measuring the change in pressure, the probe determines what the density is by using equation C-1. Table C-1 list the specifications for the density probe. The probe measures the density on the principle of specific gravity, where specific gravity is defined as

$$SG_{true} = \frac{\rho_{sample}}{\rho_{H_2O}} \quad (C-2)$$

where  $\rho_{sample}$  is the fluid that is being measured. The probe measures the temperature of the water and adjusts its water density accordingly.

**Table C-1** Cole-Palmer Low-Cost Specific Gravity Meter, 1.000 to 1.300 SGU, °C model Specifications

<b>Specifications</b>	
<b>Dimensions</b>	Meter: 4"W x 8-1/4"H x 1-1/2"D Probe: 8"L x 1-1/4" dia
<b>Specific gravity range</b>	1.000 to 1.300
<b>Specific gravity resolution</b>	0.001 SGU
<b>Specific gravity accuracy</b>	±0.004 SGU
<b>Probe immersion depth</b>	5" (12.7 cm)
<b>Temp accuracy</b>	±0.8°C
<b>Display</b>	two-line, alphanumeric LCD; backlit
<b>Max sample viscosity</b>	400 cp
<b>Temp range</b>	0 to 50°C
<b>Temp resolution</b>	0.1°C
<b>Power</b>	four AA batteries (included)

## REFERENCES

1. Sapiie, B., & Driscoll, M. J. (2009). *A Review of Geology-Related Aspects of Deep Borehole Disposal of Nuclear Wastes*. Cambridge: Massachusetts Institute of Technology.
2. Brady, P. V., Arnold, B. W., Freeze, G. A., Swift, P. N., Bauer, S. J., Kanney, J. L., et al. (2009, July). *Deep Borehole Disposal of High Level Radioactive Waste*. Retrieved May 13, 2011, from SANDIA: <http://prod.sandia.gov/techlib/access-control.cgi/2009/094401.pdf>
3. Sizer, C. G. (2006). *Minor Actinide Waste Disposal in Deep Geological Boreholes*. Cambridge: Massachusetts Institute of Technology.
4. Jensen, K. G., & Driscoll, M. J. (2010). *Technology and Policy Aspects of Deep Borehole Nuclear Waste Disposal*. Cambridge: Massachusetts Institute of Technology.
5. Marsic, N., Grundfelt, B., Wiborgh, M., & Konsult, K. (2006). *Very Deep Hole Concept Thermal effects on Groundwater Flow*. Stockholm: Svensk Kärnbränslehantering AB.
6. ChemicalLogic Corporation. (2003). *ChemicalLogic SteamTab Companion*. Burlington, MA, US.
7. Rogers, P. S., & Pitzer, K. S. (1982). *Volumetric Properties of Aqueous Sodium Chloride Solutions*. Retrieved March 17, 2011, from Journal of Physical and Chemical Reference Data: [http://jpcrd.aip.org/resource/1/jpcrbu/v11/i1/p15\\_s1](http://jpcrd.aip.org/resource/1/jpcrbu/v11/i1/p15_s1)
8. Lide, D. R. (2010). *CRC Handbook of Chemistry and Physics*. Taylor & Francis Group.
9. Dow Chemical Corporation. (2003, August 28). *Calcium Chloride Handbook: A Guide to Properties, Forms, Storage and Handling*. Retrieved May 20, 2011, from Dynalene: <http://www.dynalene.com/pdf/CalciumChloridHandbook.pdf>
10. L.Haar, et al. (1984). Appendix C. Retrieved May 15, 2011, from University of Tulsa: <http://www.personal.utulsa.edu/~kenneth-weston/appC1.pdf>